LEVEL II

(12)

A REVIEW OF AVAILABLE FREE-FIELD SEISMIC DATA FROM UNDERGROUND NUCLEAR EXPLOSIONS IN SALT AND GRANITE

INTERIM TECHNICAL REPORT

CSC-TR-78-0003

Sponsored by

ADVANCED RESEARCH PROJECTS AGENCY
ARPA ORDER NO. 02551

SEPTEMBER 1978

Prepared by

J. R. MURPHY
COMPUTER SCIENCES CORPORATION
6565 Arlington Boulevard
Falls Church, Virginia 22046

PRINCIPAL INVESTIGATOR:	J. R. MURPHY, (703) 533-8877
PROJECT SCIENTIST:	CAPT. MICHAEL J. SHORE (703) 325-8484
EFFECTIVE DATE OF CONTRACT:	OCTOBER 1, 1977
CONTRACT EXPIRATION DATE:	SEPTEMBER 30, 1978
CONTRACT NO.:	F08606-78-C-0008
PROGRAM CODE:	8F1000
AFTAC PROJECT AUTHORIZATION NUMBER:	VT/8704

A REVIEW OF AVAILABLE FREE-FIELD SEISMIC DATA FROM UNDERGROUND NUCLEAR EXPLOSIONS IN SALT AND GRANITE

INTERIM TECHNICAL REPORT

CSC-TR-78-0003

Sponsored by

ADVANCED RESEARCH PROJECTS AGENCY
ARPA ORDER NO. 02551

APPROVED FOR PUBLIC RELEASE
DISTRIBUTION UNLIMITED

CLEARED FOR OPEN PUBLICATION UNDER THE PROVISIONS OF AFR 190–17.

INFO SCTY BR., IG
AFTAC 12 OCT 78

SEPTEMBER 1978

THE VIEWS AND CONCLUSIONS CONTAINED IN THIS DOCUMENT ARE THOSE OF THE AUTHORS AND SHOULD NOT BE INTERPRETED AS NECESSARILY REPRESENTING THE OFFICIAL POLICIES, EITHER EXPRESSED OR IMPLIED, OF THE ADVANCED RESEARCH PROJECTS AGENCY, THE AIR FORCE TECHNICAL APPLICATIONS CENTER, OR THE U.S. GOVERNMENT.

Prepared by

J. R. MURPHY
COMPUTER SCIENCES CORPORATION
6565 Arlington Boulevard
Falls Church, Virginia 22046

PRINCIPAL INVESTIGATOR:	J. R. MURPHY, (703) 533–8877
PROJECT SCIENTIST:	CAPT. MICHAEL J. SHORE (703) 325–8484
EFFECTIVE DATE OF CONTRACT:	OCTOBER 1, 1977
CONTRACT EXPIRATION DATE:	SEPTEMBER 30, 1978
CONTRACT NO.:	F08606–78–C–0008
PROGRAM CODE:	8F1000
AFTAC PROJECT AUTHORIZATION NUMBER:	VT/8704

UNCLASSIFIED

SECURITY CLASSIFICATION OF THIS PAGE (When Data Entered)

REPORT DOCUMENTATION PAGE

READ INSTRUCTIONS BEFORE COMPLETING FORM

1. REPORT NUMBER: CSC-TR-78-0003	2. GOVT ACCESSION NO.
3. RECIPIENT'S CATALOG NUMBER	
4. TITLE (and Subtitle): A REVIEW OF AVAILABLE FREE-FIELD SEISMIC DATA FROM UNDERGROUND NUCLEAR EXPLOSIONS IN SALT AND GRANITE.	5. TYPE OF REPORT & PERIOD COVERED: Interim Technical Report, Covering Six Months
	6. PERFORMING ORG. REPORT NUMBER
7. AUTHOR(s): J. R. Murphy	8. CONTRACT OR GRANT NUMBER(s): F08606-78-C-0008,
9. PERFORMING ORGANIZATION NAME AND ADDRESS: Computer Sciences Corporation, 6565 Arlington Boulevard, Falls Church, VA 22046	10. PROGRAM ELEMENT, PROJECT, TASK AREA & WORK UNIT NUMBERS: ARPA Order No. 2551, Program Code 8F1000
11. CONTROLLING OFFICE NAME AND ADDRESS: Advanced Research Projects Agency/NMR, 1400 Wilson Boulevard, Arlington, VA 22209	12. REPORT DATE: September 1978 13. NUMBER OF PAGES: 58
14. MONITORING AGENCY NAME & ADDRESS (if different from Controlling Office): AFTAC/VSC, Patrick AFB, FL 32925	15. SECURITY CLASS. (of this report): UNCLASSIFIED 15a. DECLASSIFICATION/DOWNGRADING SCHEDULE

16. DISTRIBUTION STATEMENT (of this Report)

Approved for Public Release
Distribution Limited

17. DISTRIBUTION STATEMENT (of the abstract entered in Block 20, if different from Report)

18. SUPPLEMENTARY NOTES

19. KEY WORDS (Continue on reverse side if necessary and identify by block number)

Seismic, nuclear explosion, ground motion, salt, granite.

20. ABSTRACT (Continue on reverse side if necessary and identify by block number)

This report summarizes the progress that has been achieved to date in a continuing effort to compile a complete sample of free-field ground motion data from underground nuclear tests in salt and granite emplacement media. The primary objective of the study has been to collect the available data into a homogeneous data base which will serve as a useful reference for investigators who are attempting to define theoretical seismic source models for contained explosions in these two media.

(CONTINUED)

DD FORM 1 JAN 73 1473 EDITION OF 1 NOV 65 IS OBSOLETE

UNCLASSIFIED

SECURITY CLASSIFICATION OF THIS PAGE (When Data Entered)

405 727

LB

CONT'

In Chapter 2 the parameters which are typically used in the description of explosive seismic source functions are defined and some of the assumptions underlying the interpretation of measured subsurface ground motion data are critically analyzed. In particular, it is demonstrated that perturbations due to the presence of the free surface can complicate the interpretation of measurements taken above shot depth and lead to significant overestimates of the steady state value of the reduced displacement potential in some cases.

The available free-field data from the Gnome and Salmon explosions in salt and the Hard Hat, Shoal and Pile Driver explosions in granite are summarized in Chapter 3 together with the relevant geologic data describing the environment in which the measurements were made. These data include a total of 20 reduced displacement potentials: 7 from Salmon, 1 from Gnome, 4 from Hard Hat, 3 from Shoal and 5 from Pile Driver. In general, the salt data appear to be quite consistent while the granite data show large inconsistencies both between events and for different stations monitoring the same events. Various previous investigators have attributed this variability to large scale block movement in the highly fractured granites, and no better explanation seems to be available at the present time.

TABLE OF CONTENTS

LIST OF FIGURES

LIST OF FIGURES (CONT'D)

TECHNICAL REPORT SUMMARY

This report summarizes the progress that has been achieved to date in a continuing effort to compile a complete sample of free-field ground motion data from underground nuclear tests in salt and granite emplacement media. The primary objective of the study has been to collect the available data into a homogeneous data base which will serve as a useful reference for investigators who are attempting to define theoretical seismic source models for contained explosions in these two media.

In Chapter 2 the parameters which are typically used in the description of explosive seismic source functions are defined and some of the assumptions underlying the interpretation of measured subsurface ground motion data are critically analyzed. In particular, it is demonstrated that perturbations due to the presence of the free surface can complicate the interpretation of measurements taken above shot depth and lead to significant overestimates of the steady state value of the reduced displacement potential in some cases.

The available free-field data from the Gnome and Salmon explosions in salt and the Hard Hat, Shoal and Pile Driver explosions in granite are summarized in Chapter 3 together with the relevant geologic data describing the environment in which the measurements were made. These data include a total of 20 reduced displacement potentials: 7 from Salmon, 1 from Gnome, 4 from Hard Hat, 3 from Shoal and 5 from Pile Driver. In general, the salt data appear to be quite consistent while the granite data show large inconsistencies both between events and for different stations monitoring the same events. Various previous investigators have attributed this variability to large scale block movement in the highly fractured granites, and no better explanation seems to be available at the present time.

CHAPTER 1 - INTRODUCTION

A great deal of research has been conducted in recent years in an attempt to develop a firm, quantitative understanding of the magnitude/yield relations for underground nuclear explosions in a variety of source media. Such research is necessary because the process of yield estimation often involves extrapolations outside the range of current experience and this can only be accomplished with the aid of a model. This is particularly true for detonations in source media which are not normally encountered at the Nevada Test Site. For example, only two U. S. explosions (i. e. Gnome and Salmon) have been conducted in salt and these only covered the yield range from about 3 to 5 kt. Thus in order to estimate the m_b value which would be expected for say a 100 kt event in salt, it is necessary to adopt a scaling law for explosions in salt. A variety of different theoretical explosive source models have been proposed on the basis of approaches ranging from making analytic approximations to selected data from various source media (eg. Haskell, 1967) to carrying out complete nonlinear calculations using finite difference codes which incorporate equations of state designed to describe the behavior of the various source media over the entire pressure range of interest (Cherry et al, 1973). An obvious requirement of any such model is that it faithfully predict the ground motion data actually observed from explosions conducted in the medium under consideration. Unfortunately, it has not always been easy to make definitive comparisons between theory and experiment due to the fact that the published data for a given source medium are typically dispersed throughout a variety of reports which may employ different notations and systems of units.

The objective of this report is to provide a summary of the subsurface ground motion data which have been recorded from explosions in salt and granite in a form which is useful for researchers who are attempting to define the seismic source function for teleseismic compressional and surface waves. The salt and granite subsets of the data have been selected for study because reliable yield estimation for explosions in these source media can not be accomplished with confidence using the few available measured magnitude values and, consequently, extensive research is

being directed toward developing theoretical models of the response of these media to contained nuclear explosions. It should be noted that with the exception of the inclusion of a few reduced displacement potentials which have been derived since the publication of the original post shot reports, all the data presented here have been extracted from the referenced publications and simply reformatted into a more homogeneous presentation which employs a single set of units throughout. Thus, this is primarily a summary data report and attempts to interpret the observations in terms of particular models of the nuclear seismic source function have purposely been kept to a minimum.

In Chapter 2 the various parameters which are typically used in the definition of the nuclear seismic source function are defined in both the time and frequency domains. Some of the assumptions underlying the interpretation of measured subsurface data from explosions are then summarized and simple examples are presented which illustrate the difficulties associated with efforts to obtain valid free-field measurements.

The observed free-field data for the Gnome and Salmon events in salt and the Hard Hat, Shoal and Pile Driver events in granite are summarized in Chapter 3. This section includes descriptions of the geometry of the experiments, the subsurface geology at the sites, the observed peak motion data and the available derived reduced displacement potentials for each of the five events. This is followed in Chapter 4 by a summary and recommendations for further study.

CHAPTER 2 - PRELIMINARY THEORETICAL CONSIDERATIONS

Consider the one-dimensional problem of a spherically symmetric explosive source function acting in an infinite, homogeneous medium. If the detonation point is taken as the origin of a spherical coordinate system and it is assumed that there exists a spherical surface of radius r_{el} surrounding the detonation point outside of which infinitesimal strain theory is applicable, then for $r \geq r_{el}$ the equation of motion reduces to the one-dimensional wave equation in the reduced displacement potential (RDP), ϕ:

$$\frac{\partial^2 \phi}{\partial r^2} = \frac{1}{\alpha^2} \frac{\partial^2 \phi}{\partial \tau^2} \tag{2-1}$$

where α is the compressional wave velocity of the medium. Now, for outgoing spherical waves, equation (2-1) has the solution $\phi = \phi(\tau)$ where τ is the retarded time $t - (r-r_{el})/\alpha$. The radial displacement Z for $r \geq r_{el}$ is related to ϕ by

$$Z = \frac{\partial}{\partial r} \left(\frac{\phi(\tau)}{r} \right) \tag{2-2}$$

or

$$Z = \frac{1}{r^2} \phi(\tau) + \frac{1}{r\alpha} \frac{d\phi(\tau)}{d\tau} \tag{2-3}$$

Thus, given a measurement of the radial displacement at any distance $r \geq r_{el}$, the RDP can be found by integrating the differential equation (2-3) to obtain (Haskell, 1967)

$$\phi(\tau) = r\alpha e^{-\frac{\alpha}{r}\tau} \int_0^{\tau} Z(n) e^{\frac{\alpha}{r} n} dn \tag{2-4}$$

It follows from equation (2-4) that if the displacement Z at r approaches a permanent value, Z_p, as $\tau \rightarrow \infty$, then the corresponding static value of the RDP, $\hat{\phi}(\infty)$, will be given by the relation

$$\phi(\infty) = r^2 Z_p \tag{2-5}$$

Considering the relationship between displacement and RDP in the frequency domain, it follows from (2-3) that if $\hat{\phi}(\omega)$ denotes the Fourier transform of $\phi(\tau)$ and $\hat{Z}(\omega)$ denotes the Fourier transform of Z, then

$$\hat{Z}(\omega) = \left(\frac{1}{r^2} + \frac{i\omega}{r\alpha} \right) \hat{\phi}(\omega) \tag{2-6}$$

and thus the far-field ($r >> r_{el}$) displacement is given simply by

$$\hat{Z}_{FF}(\omega) = \frac{i\omega}{r\alpha} \hat{\phi}(\omega) = \frac{1}{r\alpha} \hat{\dot{\phi}}(\omega) \tag{2-7}$$

where $\hat{\dot{\phi}}(\omega)$ is the Fourier transform of the reduced velocity potential, $d\phi(\tau)/d\tau$.

In terms of the above relations it would seem to be a simple matter to define the seismic source function for underground nuclear explosions using displacement data measured beyond the region of nonlinear response. However, this has not proved to be the case, due to the fact that the environments in which the explosions take place are neither infinite in extent nor homogeneous. Consider first the perturbations introduced by the fact that the medium is bounded.

It was recognized early in the testing program that surface measurements were complicated by free surface interaction effects and thus were not well suited for defining the RDP. Consequently, programs were initiated to make measurements at depth, away from the influence of the free surface. These have come to be known as "free-field" measurements and are the subject of the present investigation. A problem arises, however, in that measurements are typically made at a variety of depths and it is not obvious which of these can be considered to be free field. While

it is not possible to provide a completely general answer to this question, some insight can be provided by considering the permanent displacement field produced by an explosive source in an elastic halfspace. With reference to Figure 2-1, if h is the source depth, Z the receiver depth and r is the horizontal distance between source and receiver, then it can be shown that the permanent displacement will be given by (Tien and Hadsell, 1970)

$$\tilde{Z}_p = \frac{\phi(\infty)}{\sin I} \left[- \frac{\sin I}{R^2} - \frac{3h \sin 2I'}{R'^3} + \frac{\sin I' (1 + 3 \cos 2 I')}{R'^2} \right] \tag{2-8}$$

where

$$R = \sqrt{(h - z)^2 + r^2}$$
$$R' = \sqrt{(h + z)^2 + r^2} \tag{2-9}$$

$$\text{Sin } I = r/R$$
$$\text{Sin } I' = r/R'$$

On the other hand, for an infinite, homogeneous medium it follows from equation (2-5) that

$$Z_p = \frac{\phi(\infty)}{R^2} \tag{2-10}$$

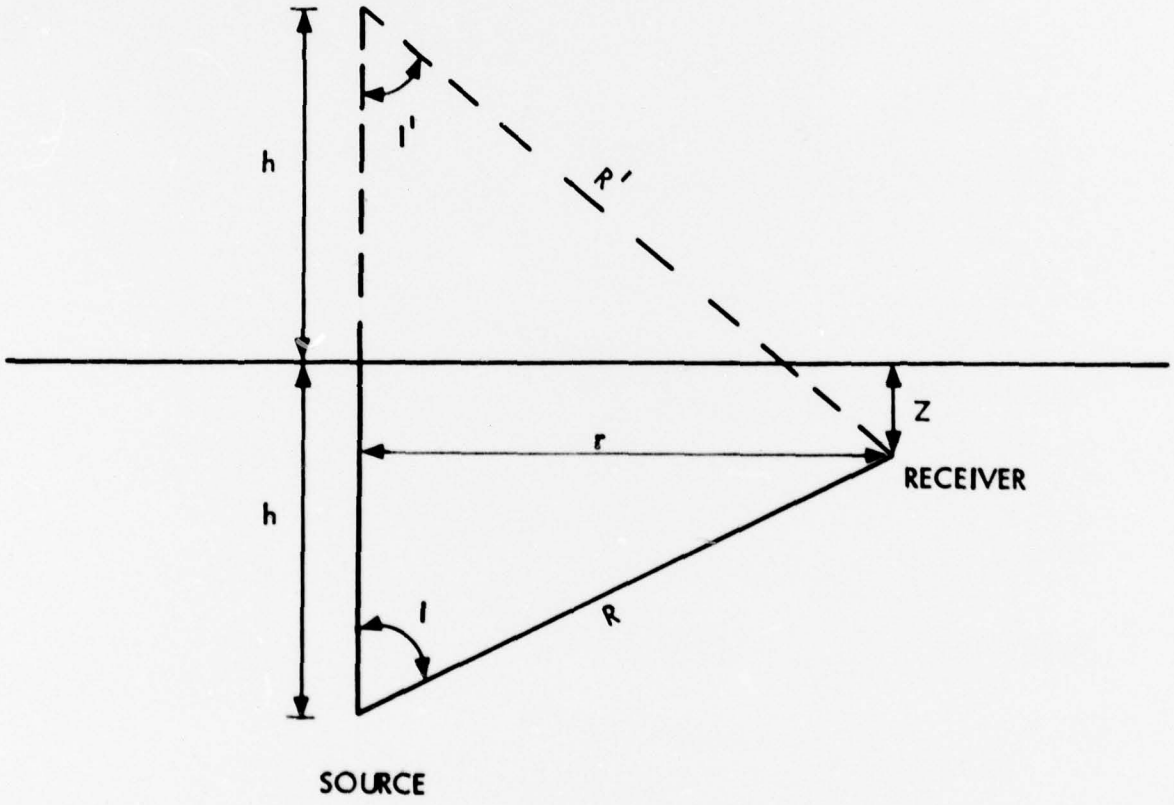

Figure 2-1. Geometry of the Halfspace Model

The ratio $\tilde{Z}_p / Z_p$ (i.e. halfspace/fullspace) is shown as a function of receiver depth in Figure 2-2 for the case r = 2h. It can be seen that the perturbation due to the free surface produces an amplification effect which extends to fairly great depth. In fact, in this case, the displacement in the halfspace at one half the source depth is still 1.75 times that which would be expected at that distance in an infinite homogeneous medium. Thus, the interpretation of measurements made significantly above source depth will be subject to uncertainty. For this reason, the present investigation focuses primarily on data measured near shot depth.

Effects due to departures from homogeneity will no doubt depend upon the details of the subsurface geologic structure in the vicinity of the explosion being considered. However, the Salmon event has been selected to illustrate these effects because this is one of the few events for which a large variety of high quality free field data have been measured in a region where the local geology is well known. Figure 2-3 shows the locations of the subsurface instruments relative to the geologic structure of the salt dome and the overlying formations. Although all the instruments are located in salt, it is clear that the medium is not even approximately homogeneous with the salt/anhydrite boundary lying only a few hundred meters above the shot point. The question then is whether such a layered source medium can be expected to significantly modify the measurements taken at source depth from what would be expected in a homogeneous medium. Figure 2-4 shows a comparison of the Salmon vertical acceleration records taken at source depth at ranges of 318 and 744 m (Perret, 1968a). For a spherically symmetric source in an infinite homogenous medium, these components of motion would be expected to be identically zero and, in fact, their amplitude levels are very small relative to those associated with the corresponding radial component motions. However, the point of interest here is that the apparent duration and complexity of the signal clearly increases with increasing distance. This is typical of free field measurements and suggests that reflections of the primary pulse from nearby inhomogeneities are indeed contributing to the motion at shot depth.

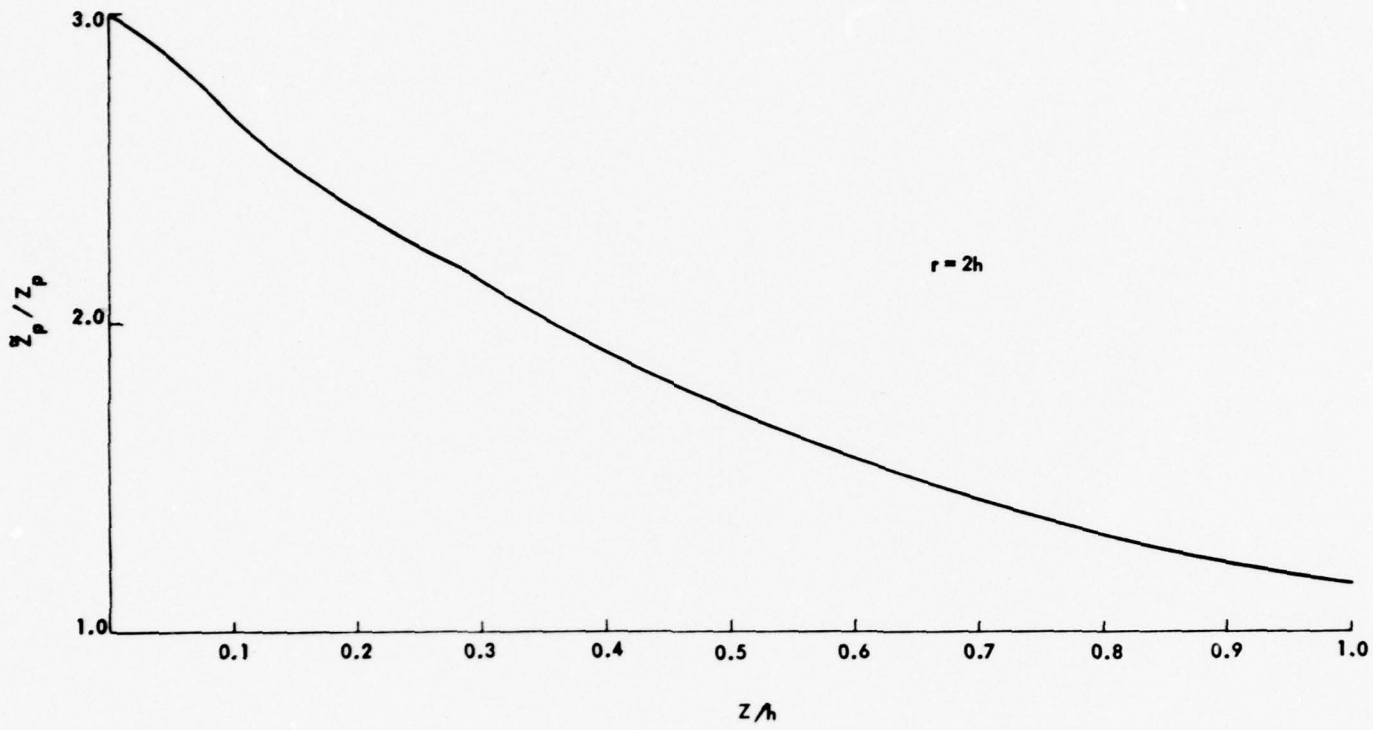

Figure 2-2. Theoretical Ratio of Halfspace to Fullspace Permanent Radial Displacements as a Function of Normalized Receiver Depth, r = 2h

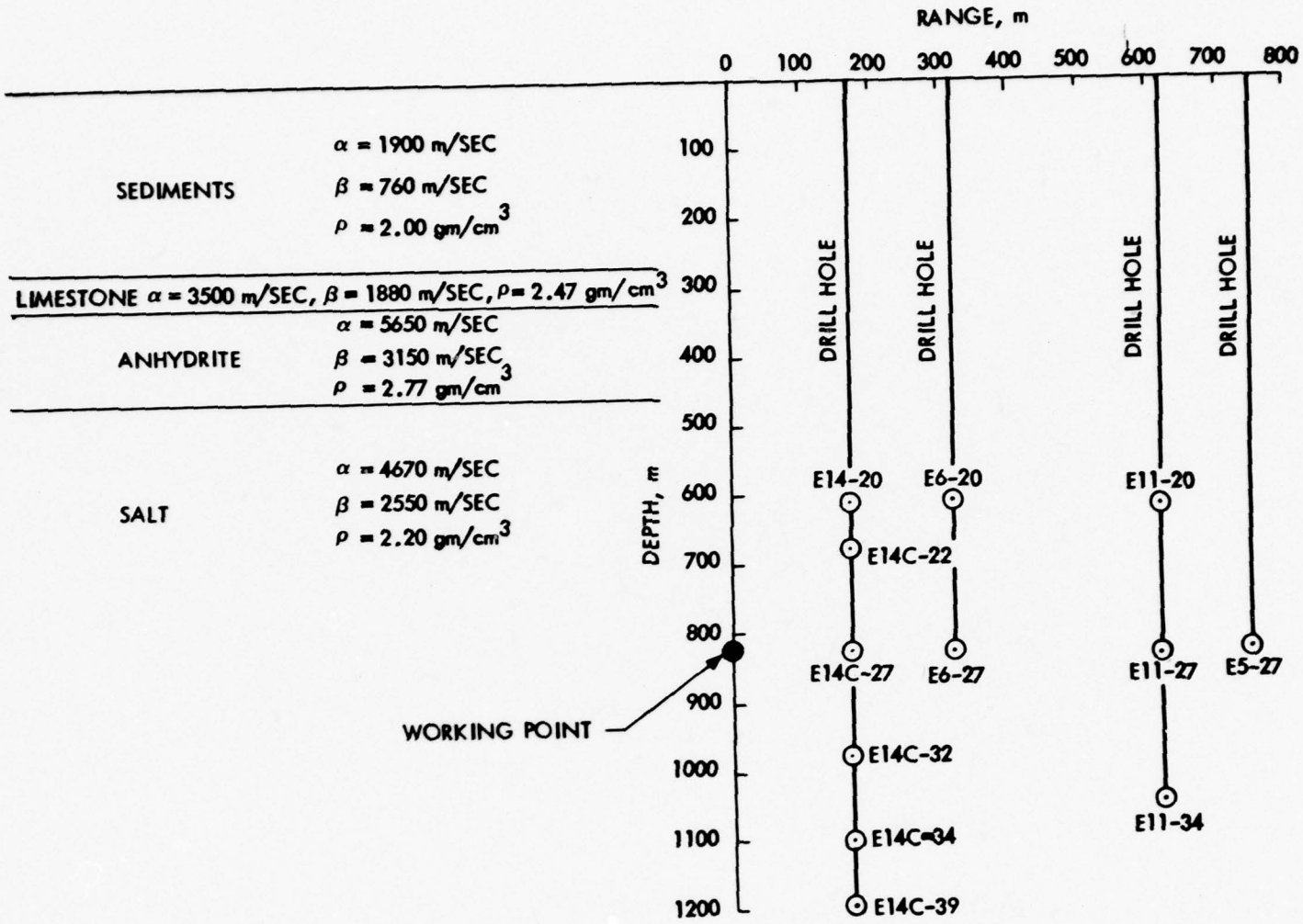

Figure 2-3. Vertical Section Through the Salmon Detonation Point Showing the Relationship Between the Instrument Locations and the Subsurface Geology at the Site

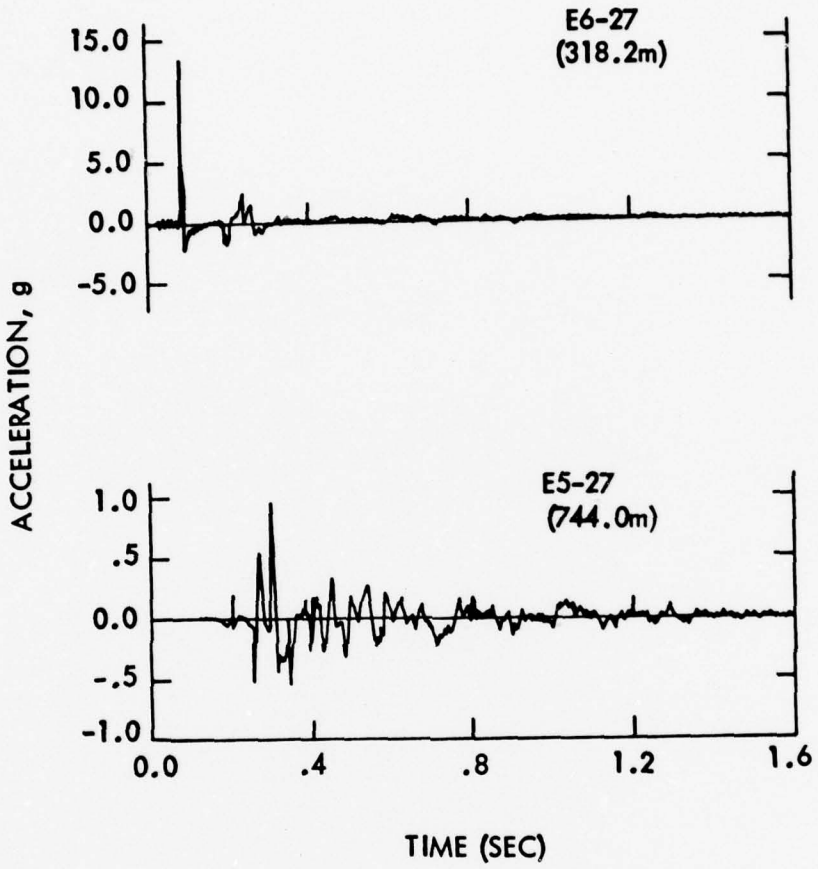

Figure 2-4. Comparison of the Salmon Vertical Acceleration Records Taken at Source Depth at Ranges of 318 and 744 m

That is, at the longer ranges the travel paths associated with indirect reflected arrivals are more nearly equal to those of the directly induced motion and consequently their amplitudes are comparable. This would give rise to an increasing complexity with increasing range such as that illustrated in Figure 2-4.

In order to evaluate the magnitude of the influence of these secondary arrivals on the observed RDP, it is necessary to consider the effects of specific arrivals on the observed radial components of motion. Figure 2-5 shows a comparison of the horizontal components of acceleration measured 200 m above (E11-20) and below (E11-34) the shot elevation at a range of about 650 m (Perret, 1968). It can be seen from this figure that the initial arrival is remarkably consistent on the two records with regard to both amplitude level and shape, indicating that the primary radiation for this event is very nearly spherically symmetric. However, on the record taken at station E11-20 there is a clear indication of a secondary arrival which appears to have no counterpart on the record taken at the deeper station E11-34. An examination of the geologic structure shown in Figure 2-3 suggests that this arrival may be a reflection from the salt/anhydrite interface which follows the travel path indicated in Figure 2-6. The expected magnitude of this arrival at the two stations can be estimated by considering the differences in the reflection coefficients at the boundary and the relative attenuation due to differences in travel path. The P wave reflection coefficient (Murphy, 1972) has been evaluated for the two stations using the measured physical property contrast between salt and anhydrite and the angles of incidence shown in Figure 2-6. It was found to be about 0.2 for station E11-34 and about 0.5 for station E11-20. The corresponding total path lengths for this arrival to stations E11-34 and E11-20 are about 1130 and 815 m respectively. Thus, if the amplitude of the direct arrival is A, the amplitude of the reflected arrivals should be given approximately by

$$A'_{E11-20} = A \cdot (0.5) \cdot \left(\frac{650}{815}\right)^3 \cdot \cos 40^\circ \simeq 0.20\,A$$

$$A'_{E11-34} = A \cdot (0.2) \cdot \left(\frac{650}{1130}\right)^3 \cdot \cos 60^\circ \simeq 0.02A$$

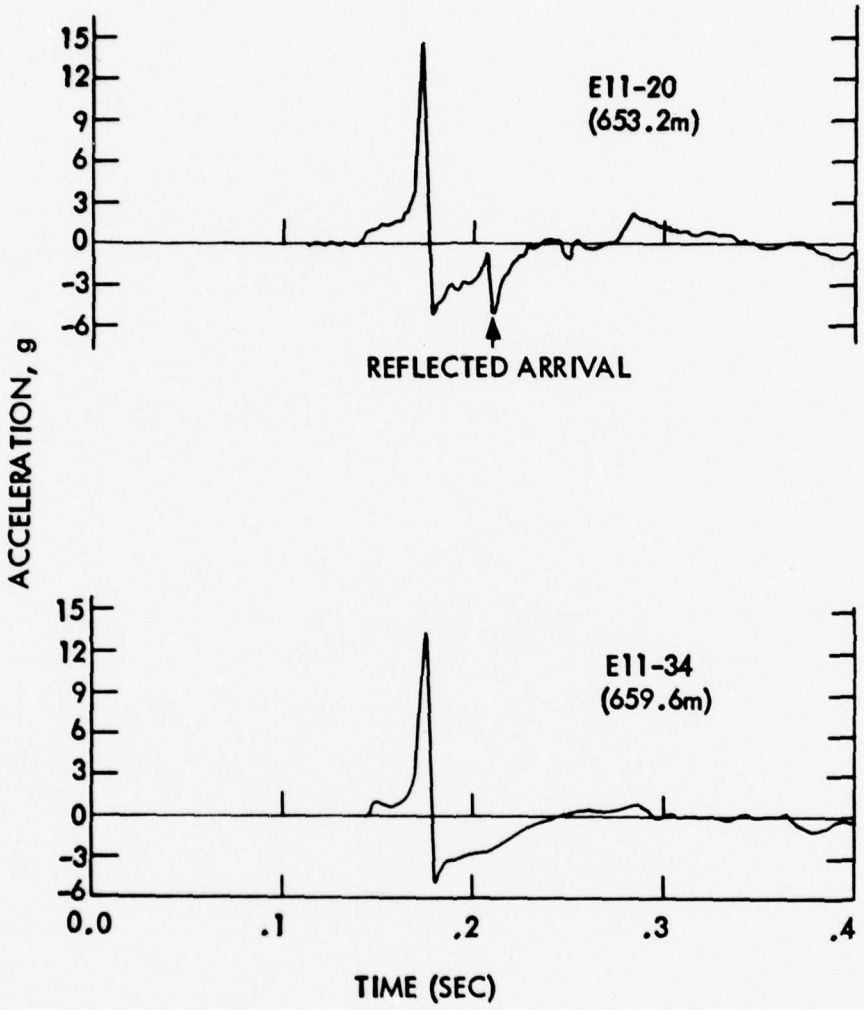

Figure 2-5. Comparison of Radial Acceleration Records Measured 200 m above (E11-20) and Below (E11-34) the Salmon Shot Depth at a Range of 650 m

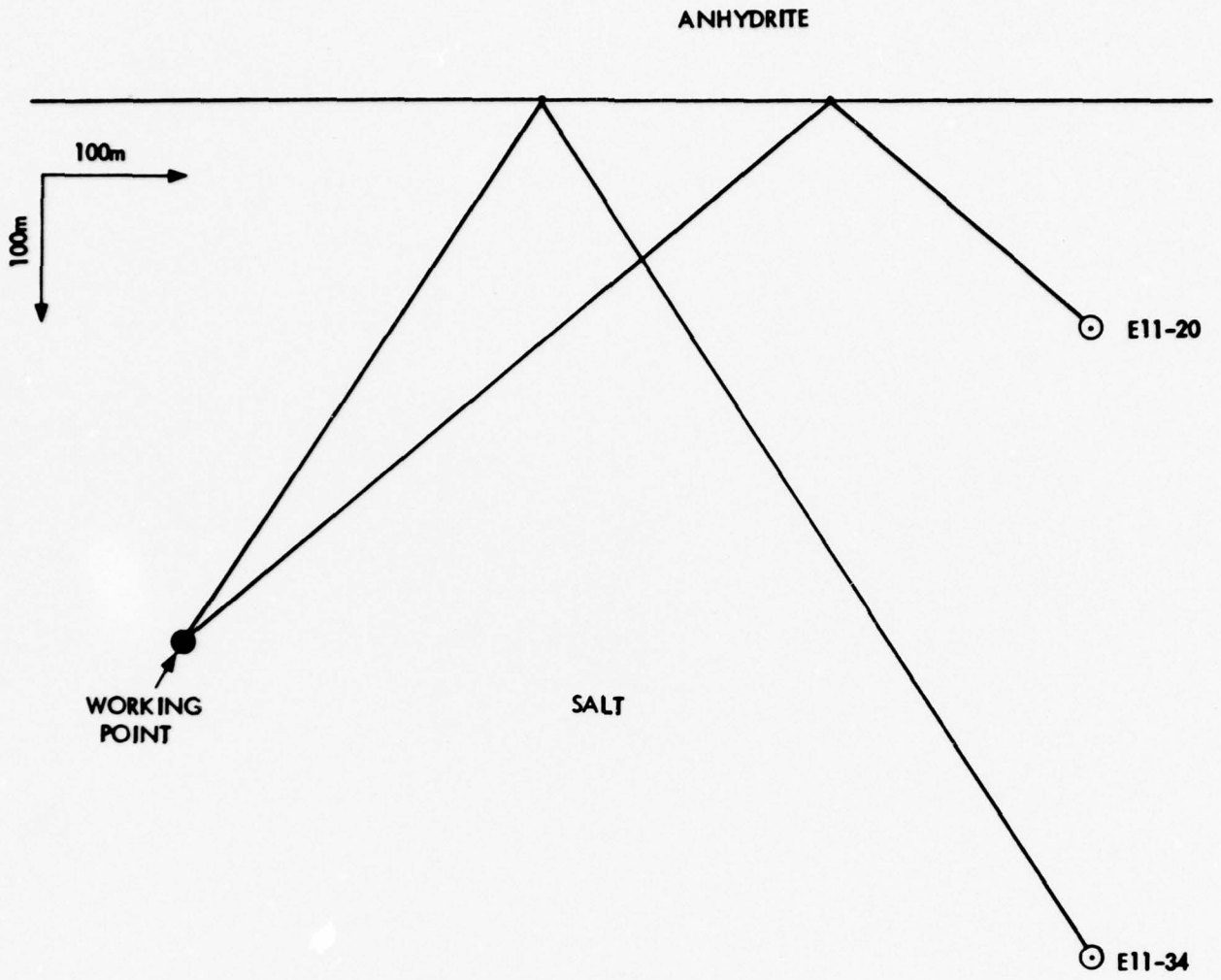

Figure 2-6. Comparison of the Travel Paths of the Reflections from the Salt/ Anhydrite Boundary to Salmon Stations E11-20 and E11-34

where the experimentally observed R^{-3} range dependence of peak acceleration for Salmon (Perret, 1968a) has been assigned and the cosine terms have been incorporated to account for projection of the reflected motion onto the horizontal axis. Thus, the reflected arrival is expected to be an order of magnitude smaller at station E11-34 than at station E11-20, in agreement with the observed differences in the records from these stations shown in Figure 2-5. More specifically, the observed ratio of reflected to direct amplitude (i.e. A'/A) at station E11-20 is about 0.2 and the difference in arrival time is about 0.035 seconds, in excellent agreement with what would be expected for the P wave reflection from the salt/anhydrite boundary. This same arrival is also evident on the vertical acceleration record at station E6-27 shown previously in Figure 2-4. In fact, a detailed analysis of this record indicates the presence of two later arrivals which can be quantitatively correlated with respect to both amplitude and phase with expected reflections from the overlying anhydrite/limestone and limestone/sediment boundaries (cf. Figure 2-3).

Thus the evidence is clear that reflections from nearby heterogeneities do perturb the motion measured at shot depth from that which would be expected in a homogeneous medium. For the Salmon event, these secondary contributions to the observed radial components of motion appear to be small relative to that of the directly induced motion. However, it seems likely that the relative importance of such secondary arrivals will increase with increasing range. Thus, there is a basic conflict in that it is desireable to be at large enough range to insure being outside the nonlinear regime and, at the same time, close enough that the homogeneous approximation is appropriate. For this reason, free-field data collected in the vicinity of the estimated elastic radius will be given more weight in the present investigation than the subsurface data measured at much greater distances.

CHAPTER 3 - MEASURED FREE FIELD DATA FROM EXPLOSIONS IN SALT AND GRANITE

3.1 OVERVIEW

In this section the free-field data from the Salmon and Gnome events in salt and the Shoal, Hard Hat, and Pile Driver events in granite will be reviewed and summarized. Wherever necessary, the originally reported values have been converted to a common system of units: range and depth in meters; peak particle accelerations, velocities, and displacements in g, cm/sec and cm respectively; RDP in m^3. For each event the following information is provided: (1) a surface map of the site showing the geometry of the experiment, (2) a vertical section through the detonation point showing the relationship between the instrument locations and the local subsurface geology, (3) displays of the available free-field peak motion data and (4) displays of the currently available RDP's which have been derived from the measured ground motion data by a number of different investigators. It should be noted that with a few exceptions, the RDP's shown below are simply redrafted versions of the figures presented in the referenced reports, converted to a common set of units (i.e. m^3), and thus are not suitable as input to digital processing. However, enough care has been taken in their reproduction to insure that the rise time, peak amplitude and steady state amplitude are accurate to within a few percent.

A review of the published experiment descriptions indicates that all the data to be described below were recorded on instruments which are characterized by a flat response over the seismic frequency range of interest (i.e. < 20 Hz). Moreover, all of the downhole instruments were set in place using specially designed grout with physical properties approximately equal to those of the surrounding medium. Thus, no instrument corrections are required and it will be assumed in the following that the recorded data are faithful reproductions of the actual ground motions.

3.2 SALMON

The Salmon event was a 5.3 kt contained explosion which was detonated at a depth of 828 m ($h/W^{1/3}$ = 475) in the Tatum salt dome in Mississippi on October 22, 1964. The subsurface ground motion data collected on this experiment are easily the most complete and consistent set which are currently available. Twelve subsurface locations at slant ranges between 167 and 740 m were instrumented and high quality data were recorded on the majority of the 49 accelerometers and velocity meters deployed at these sites. These data indicate a high degree of symmetry and consistency and thus can be used to define a relatively confident estimate of the RDP for this event.

Figure 3-1 is a surface map of the site (Perret, 1968a) which shows the relationship between the emplacement hole, the instrument holes and the upward projection of the boundary of the salt dome at shot depth. It can be seen from this figure that none of the stations is close enough to the dome boundary that lateral reflections would be expected to significantly contribute to the observed radial motion. Figure 3-2 shows all the downhole instrument locations projected onto a single vertical plane through the shot point. The subsurface geologic profile shown to scale on the left side of this figure provides an indication of the local variation in physical properties in the medium surrounding the observation points. It was noted previously in Chapter 2 that the effect of these horizontal discontinuities on the observed radial motion in the salt is expected to be small, at least over the distance range of interest here.

The observed peak radial accelerations, velocities and displacements are shown as a function of slant range in Figure 3-3 (Perret, 1968a). The solid lines on these figures represent the least-squares fit to the data proposed by Perret (1968a). It can be seen that in each case the data are quite consistent with a simple power law dependence on distance, with the higher frequency peak accelerations showing the most rapid attenuation with distance (i.e. $R^{-2.94}$) and the lower frequency displacements attenuating most slowly (i.e. $R^{-1.58}$) as expected.

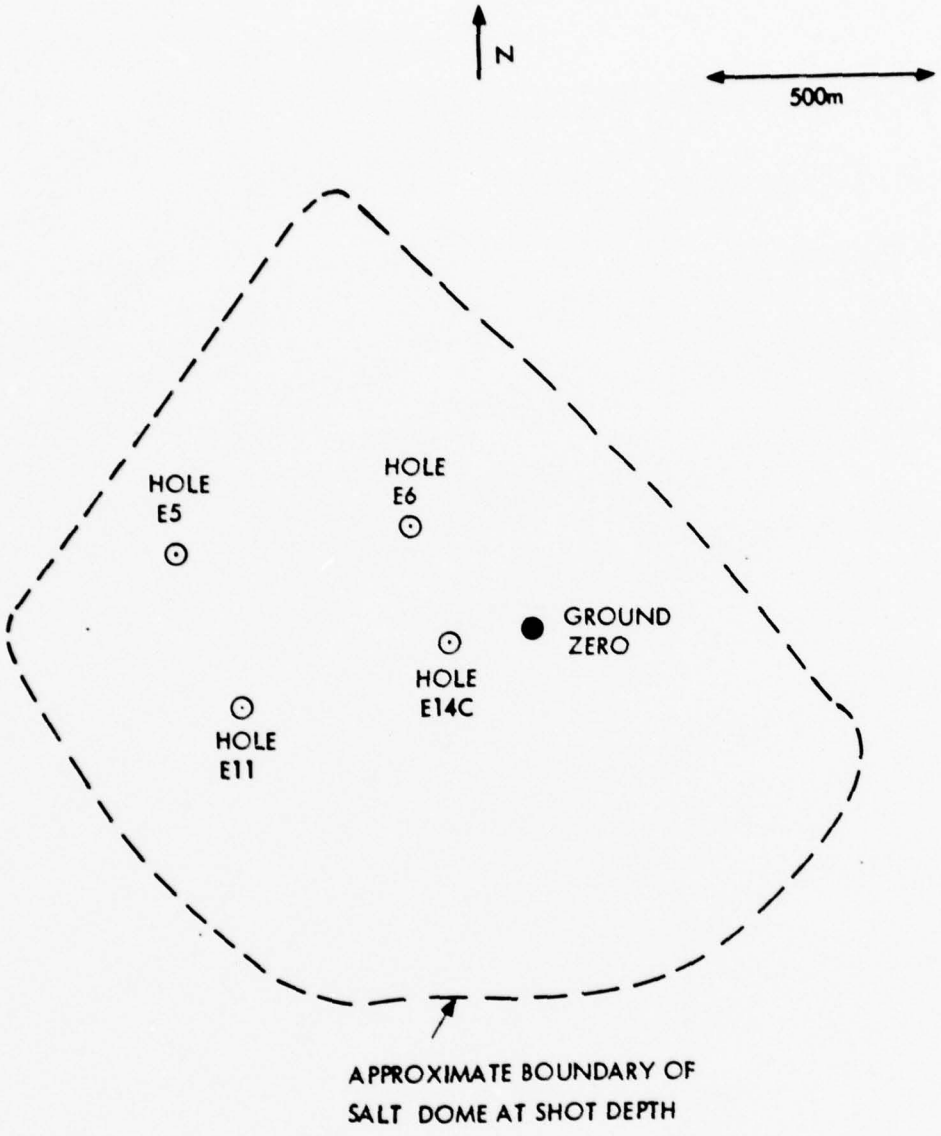

Figure 3-1. Surface Map of the Salmon Site

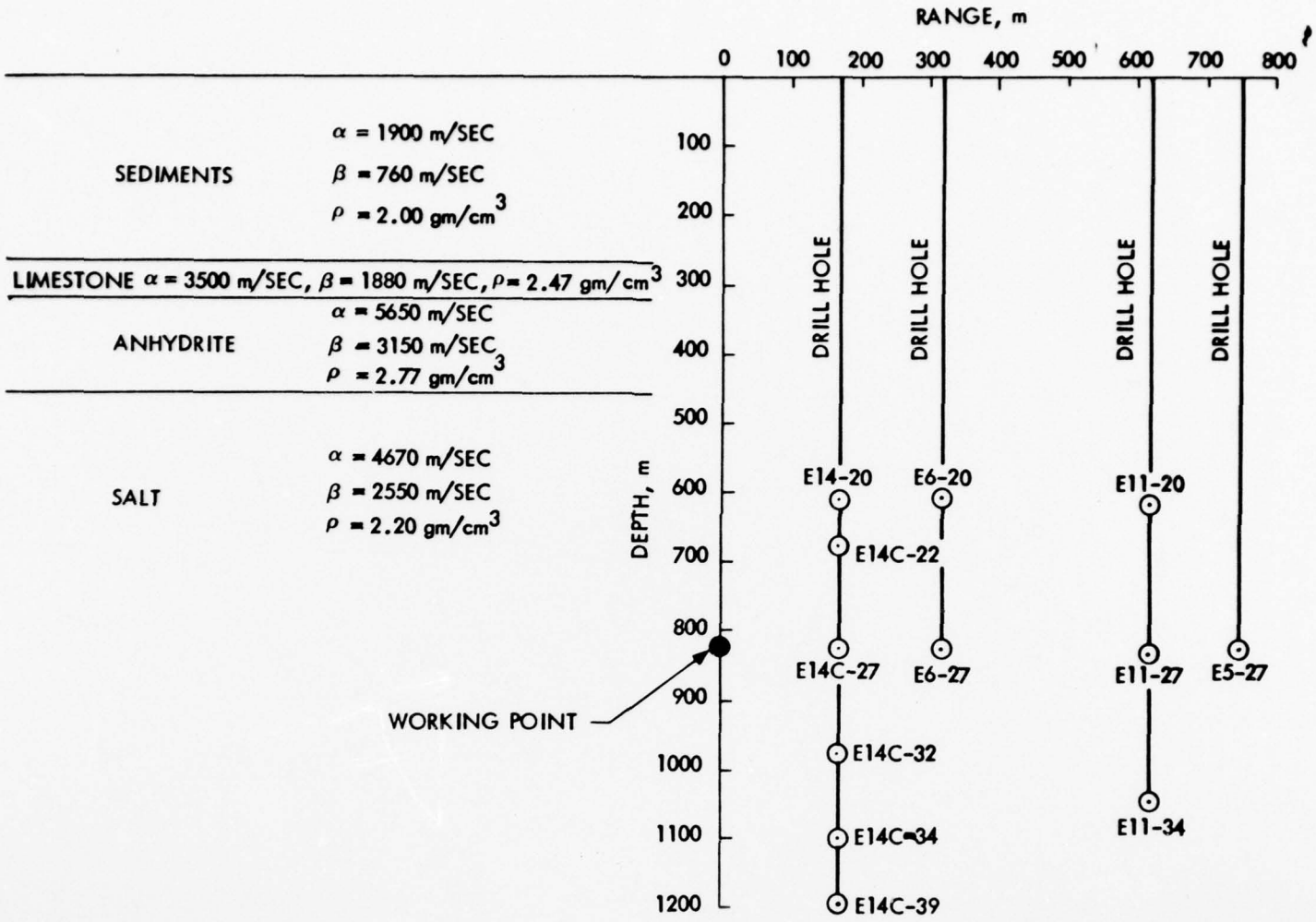

Figure 3-2. Vertical Section Through the Salmon Detonation Point Showing the Relationship Between the Instrument Locations and the Subsurface Geology at the Site

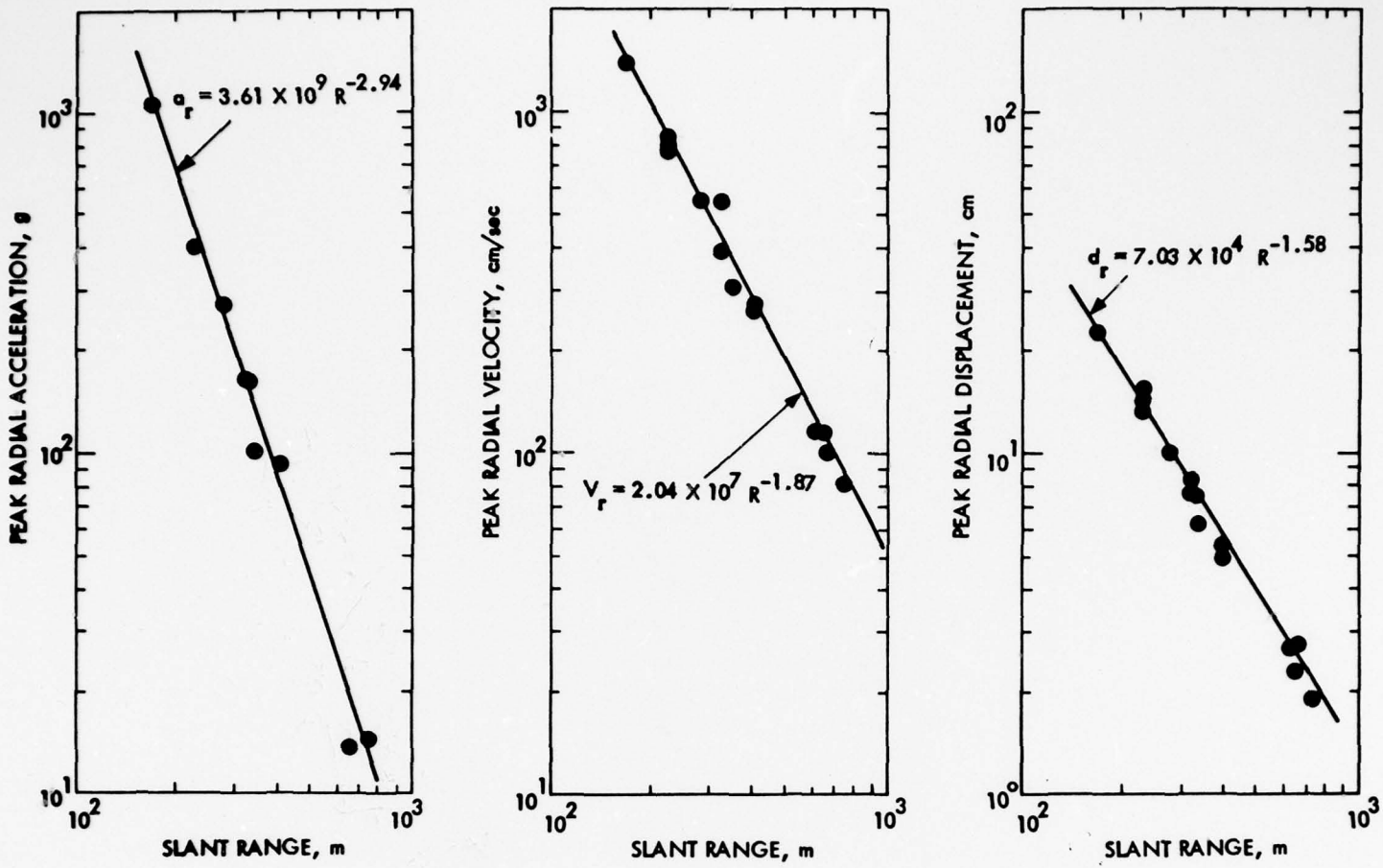

Figure 3-3. Observed Salmon Peak Motion Data as a Function of Range

Reduced displacement potentials have been derived from virtually every Salmon recording. Perret (1968a) lists potential peaks and residual values for each of the 12 stations and Rogers (1966) lists potential peaks and residual values obtained from some 57 directly measured and derived recordings. However, complete RDP's plotted as a function of time have been published for only 7 of these records (Perret, 1968a; Patterson, 1966). These seven time histories are reproduced on a common scale in Figures 3-4 and 3-5. A compressional wave velocity (α) of 4670 m/sec was assumed in deriving these RDP's (Perret, 1968a), consistent with the propagation velocity actually observed for the Salmon data. As would be expected on the basis of the other observed ground motion parameters, the RDP's shown in Figures 3-4 and 3-5 are quite consistent and indicate a peak value of the potential of between 4,000 and 5,000 m^3 and a steady state value of the potential predominantly in the 3,000 to 4,000 m^3 range. Springer (1966) on the basis of his review of all the RDP data concluded that the potential from station E11-27 was representative of those measured in the elastic regime. As is shown on Figure 3-5, this RDP has a peak of about 4,000 m^3 and a steady state value of about 3,000 m^3.

3.3 GNOME

The Gnome event was a 3.1 kt contained explosion which was detonated at a depth of 366 m ($h/W^{1/3}$ = 250) in a stratified salt medium near Carlsbad, New Mexico on December 10, 1961. Ground motion measurements were made at 12 different shot level stations; 7 in a tunnel and one at the bottom of a hole along a line striking about S50^{o}W from the shot point and 4 at the bottom of individual drill holes extending out on a line striking about N5^{o}E from ground zero. The 8 stations along the S50^{o}W line were distributed over a distance range from 62 to 477 m and were the responsibility of investigators from Sandia Corporation (SC; Weart, 1963). The 4 downhole stations along the N5^{o}E line were distributed over the distance range from 805 to 9450 m and were the responsibility of investigators from Stanford Research Institute (SRI; Swift, 1963). Although good data were recovered from this experiment, cable damage limited the operating time of most of the instruments and, consequently, the late time response was not well determined in many cases.

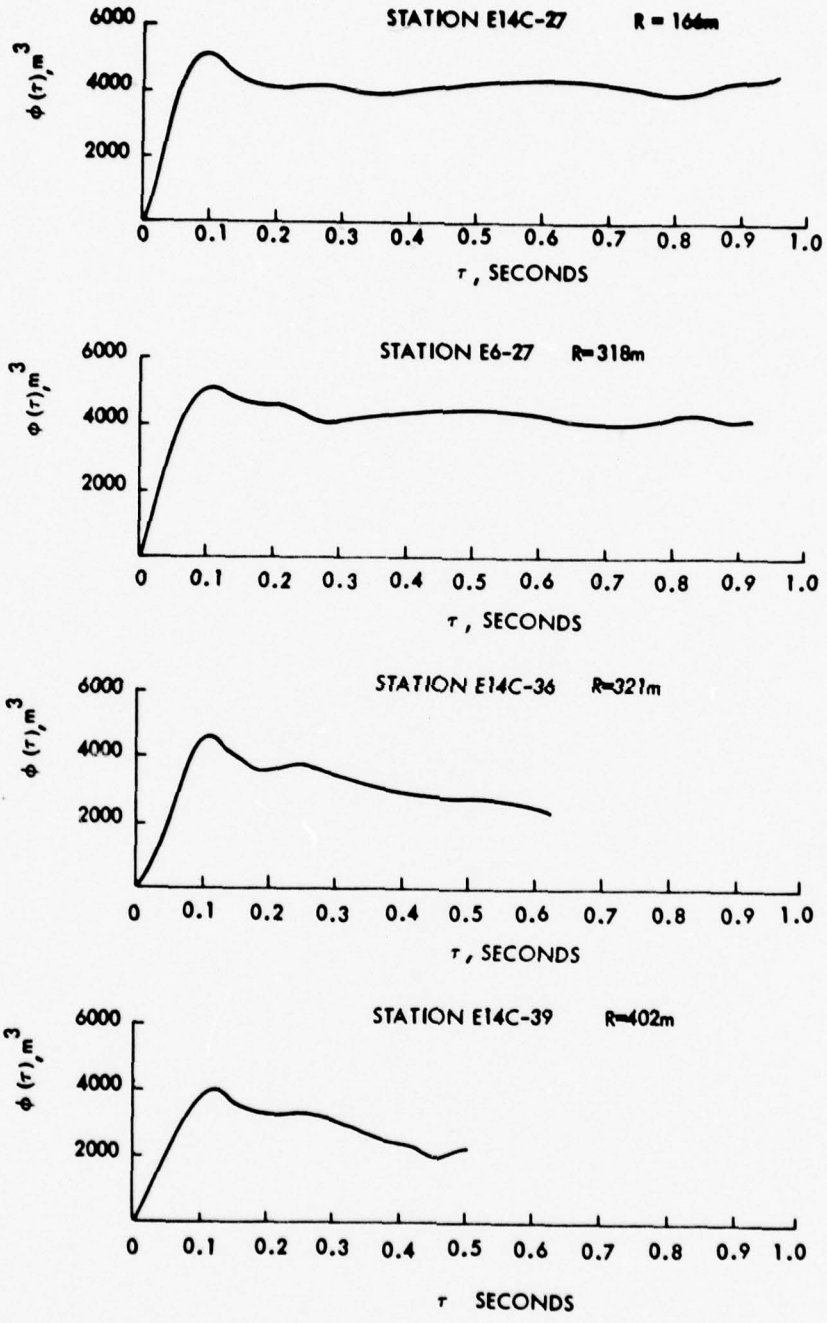

Figure 3-4. Observed Salmon Reduced Displacement Potentials, Stations E14C-27, E6-27, E14C-36 and E14C-39

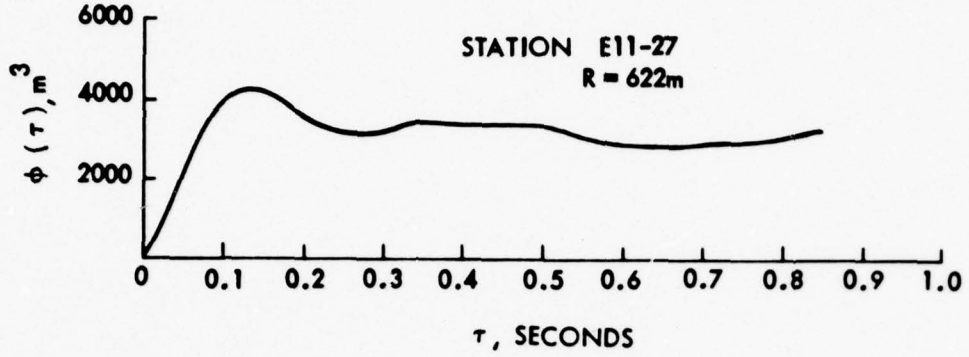

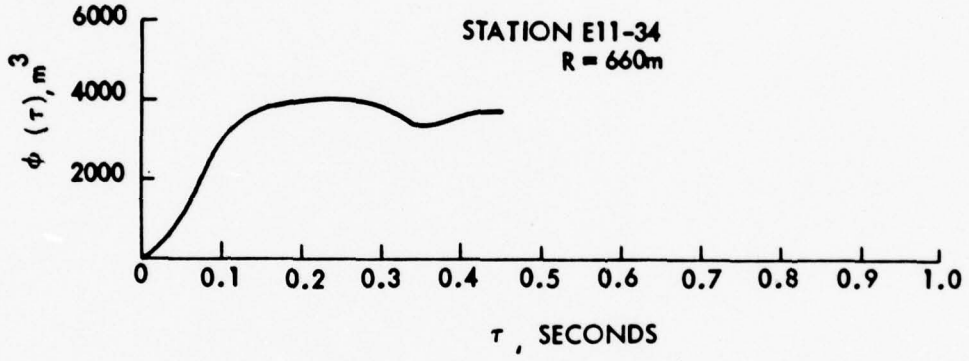

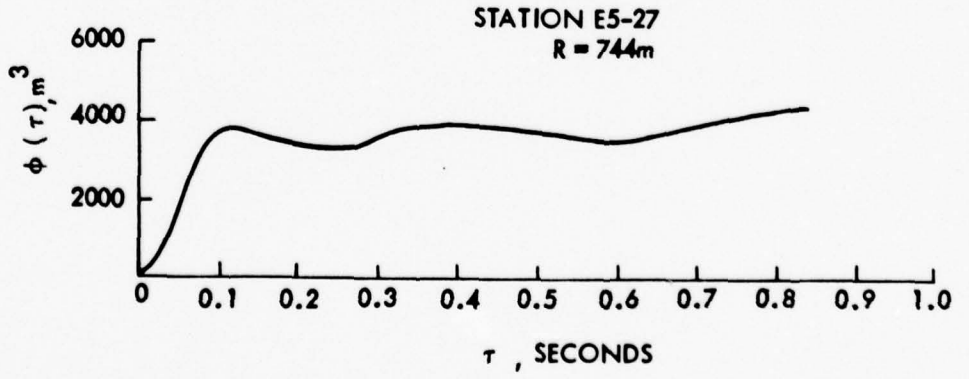

Figure 3-5. Observed Salmon Reduced Displacement Potentials, Stations E11-27, E11-34 and E5-27

Figure 3-6 is a surface map of the site (Weart, 1963; Swift, 1963) which shows the location of the tunnel access shaft, the SC instrument hole and three of the four SRI instrument holes with respect to ground zero. The remaining SRI station is located off this map nearly 10 km north of ground zero. As might be expected on the basis of the discussion in Chapter 2, the recordings at this station, and also at stations SRI 4 (R = 3.2 km) and SRI 3 (R = 1.6 km), are quite complex and of long duration and seem to bear no simple relationship to the directly induced motion measured at the closer-in stations. For this reason, the data recorded at these stations will not be considered further in the present analysis. The subsurface locations of the remaining 9 stations are shown projected onto a vertical plane through the shot point in Figure 3-7. The subsurface geologic profile shown to scale on the left side of this figure is based on data measured directly over the shot point (Weart, 1963). However, available evidence (Weart, 1963; Swift, 1963) suggests that the near surface geology is fairly uniform across the area overlying the station locations shown on this figure. In this case, only the compressional wave velocities (α) of the overlying media have been experimentally determined and consequently no estimates of the shear wave velocities and densities are currently available for these units.

The peak radial acceleration, velocity and displacement data observed at ranges greater than 100 m are plotted as a function of distance in Figure 3-8. The data measured at the closer-in distances are not shown on this figure both because they are incomplete due to cable damage and also because they are characteristic of the strongly nonlinear propagation range which is not of interest in the present investigation. In Figure 3-8, the solid circles denote the SC measurements, the open circles the SRI measurements and the solid lines are the least squares fit to the SC data measured at distances greater than 100 m (Weart, 1963; Swift, 1963). It can be seen that the observed SRI data agree fairly well with the extension of the SC best-fit attenuation line, and since these measurements were made along radii differing by about 135° in azimuth, Swift (1963) has interpreted this as an indication of a spherically symmetric source function.

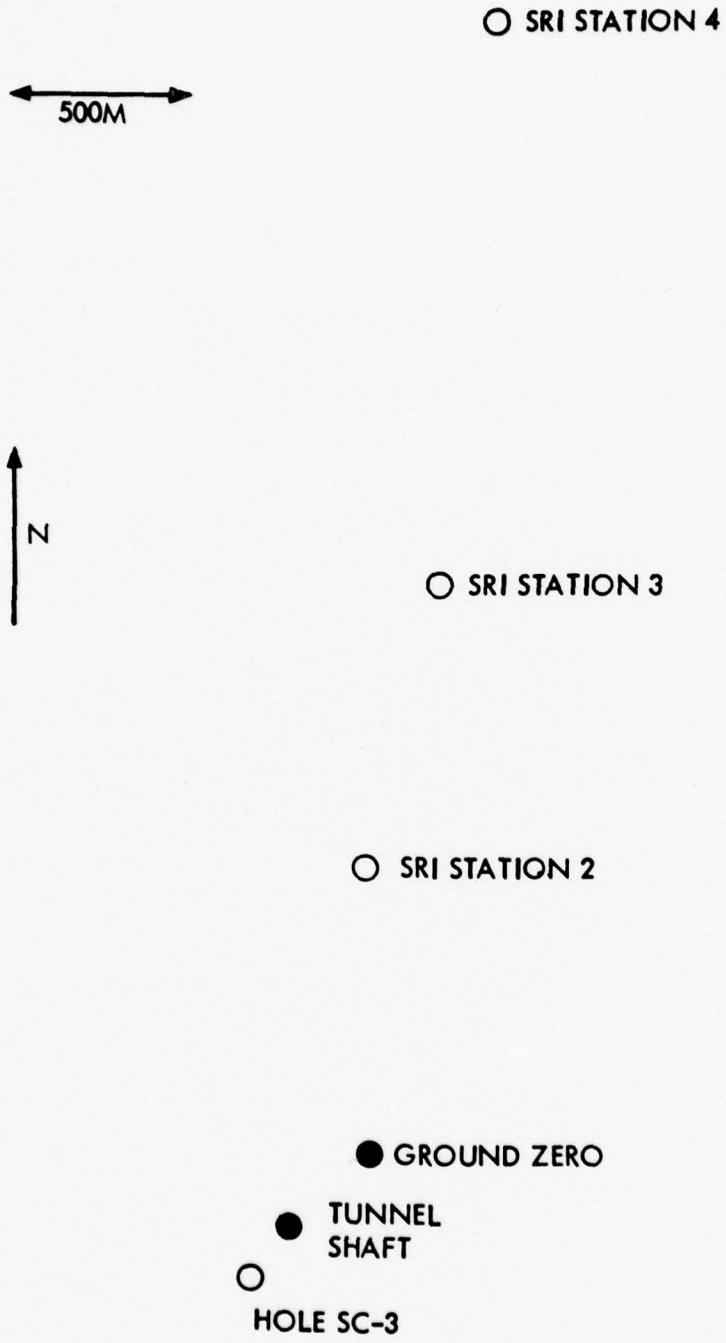

Figure 3-6. Surface Map of the Gnome Site

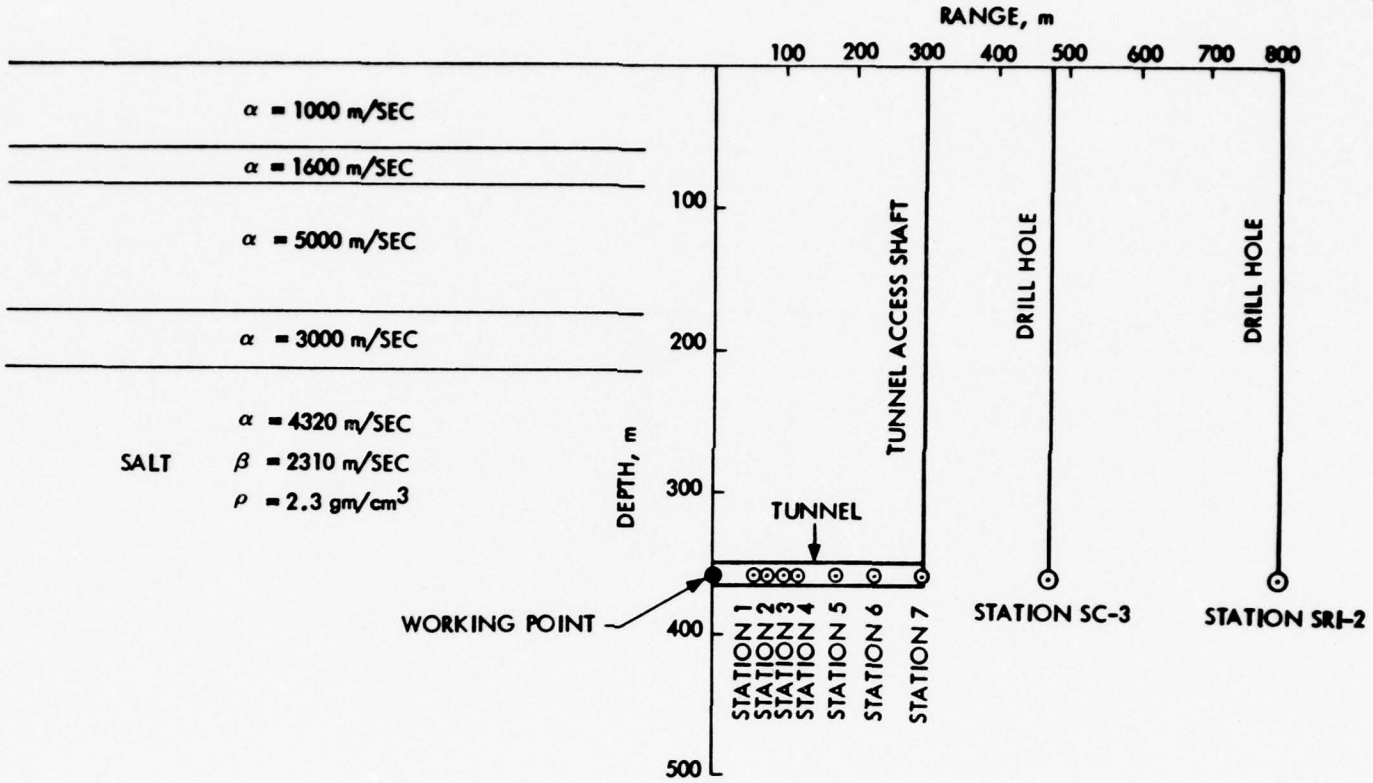

Figure 3-7. Vertical Section Through the Gnome Detonation Point Showing the Relationship Between the Instrument Locations and the Subsurface Geology at the Site

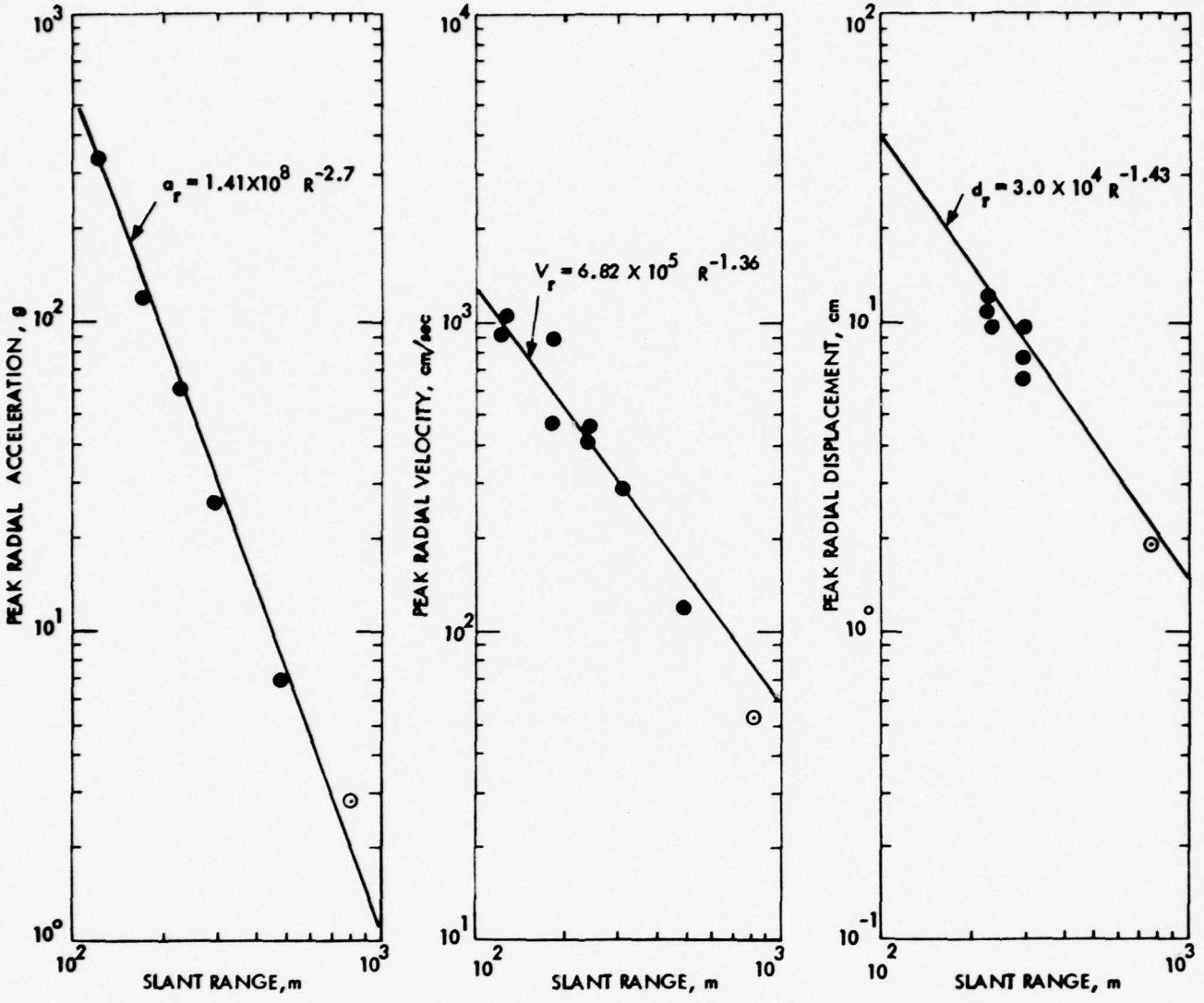

Figure 3-8. Observed Gnome Peak Motion Data as a Function of Range

Reasonably complete radial component time histories of motion were recorded in the tunnel at a range of 298 m and downhole at stations SC-3 (R = 467m) and SRI-2 (R = 805m). However, only the tunnel record of velocity at a range of 298 m has been integrated to obtain an estimate of the RDP for Gnome (Werth and Herbst, 1962). In deriving this RDP, Werth and Herbst (1962) used the estimated pre-shot compressional wave velocity of 4080 m/sec instead of the observed Gnome propagation velocity of 4320 m/sec. Since the choice of α influences the derived RDP (Cf. equation (2-41)), the RDP's estimated using both values of α are presented in Figure 3-9. It can be seen from this figure that the variation due to this small change in α is negligible and that the observed ground motion data are consistent with a peak potential value of about 4500 m^3 and a steady state value of about 3100 m^3.* Werth and Herbst (1962) indicate that this derived value of $\phi(\infty)$ is consistent with the estimated size of the Gnome cavity before roof fall under the usual simplifying assumption of incompressibility.

3.4 HARD HAT

The Hard Hat event was a 5.9 kt contained explosion which was detonated at a depth of 290 m ($h/W^{1/3}$ = 160) in the granite of Climax stock in Area 15 of the Nevada Test Site (NTS) on February 15, 1962. Twelve subsurface stations at or below shot level were occupied for this event; 6 in a tunnel striking approximately due south of the detonation point and 6 more at the bottom of individual holes located approximately north, south, east, and west of ground zero. The 6 tunnel stations were logarithmically spaced over the distance range from 78 to 244 m and were the responsibility of SC (Perret, 1963). The downhole stations were located at distances of 305 and 457 m and were the responsibility of SRI (Swift, 1962). Thus the instrumentation plan for

---

*In comparing the RDP in Figure 3-9 with that presented by Werth and Herbst (1962), it should be noted that those authors cube-root scaled their derived Gnome RDP to 5 kt using the initial post shot yield estimate of 3.5 kt.

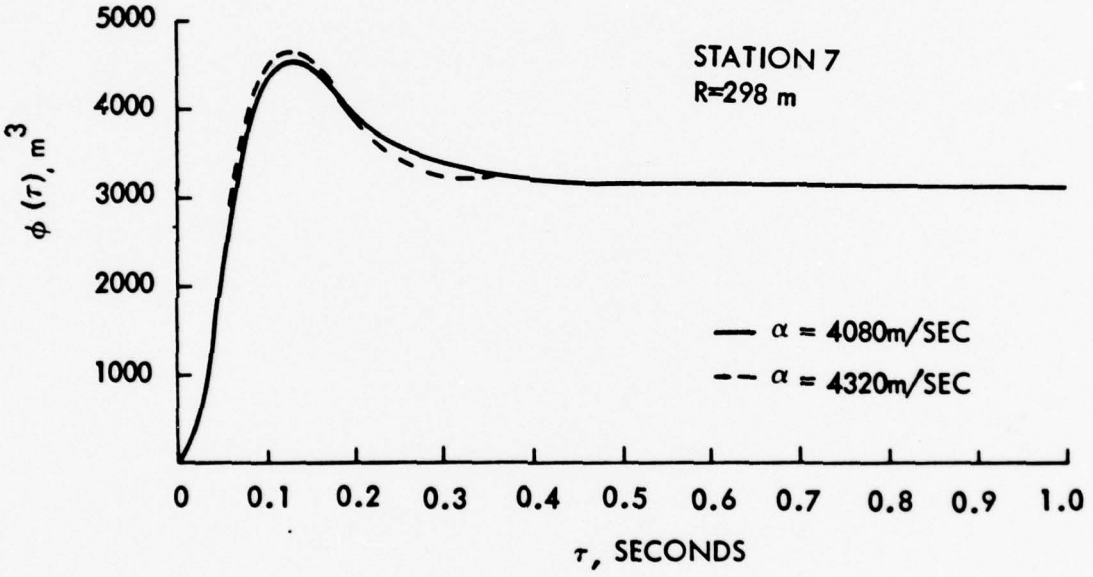

Figure 3-9. Observed Gnome Reduced Displacement Potential, Station 7

this event was quite elaborate. Unfortunately, however, only about 50% of the potential data were recovered due to a variety of problems and many of these data were terminated prematurely due to cable breaks and recorder damage at the instrumentation trailer.

A surface map of the site is shown in Figure 3-10 which indicates the relationship between the locations of ground zero, the tunnel access shaft and the individual instrument holes. The subsurface locations of these stations are shown projected onto a vertical plane through the shot point in Figure 3-11. It can be seen from this figure that the two stations SRI-1 and SRI-2 are located well below shot depth along a radius inclined about 50° below the horizontal. These stations were designed to monitor the outgoing motion along a take-off angle representative of propagation to teleseismic distances. The subsurface geologic profile shown on the left of this figure is a rough approximation in that the granite is mapped as a single unit outcropping at the surface. However, the data recorded near the surface from Hard Hat suggest the existence of a thin layer of low velocity weathered granite (Swift, 1962) compatible with that indicated here.

The peak radial acceleration, velocity and displacement data observed at ranges greater than 100 m are plotted as a function of distance in Figure 3-12. As in previous figures, the SC values (Perret, 1963) are shown as solid circles and the SRI values (Swift and Eisler, 1965) as open circles. Since the SRI values were revised after the publication of Perret's report (1963), the least squares fit solid lines on these figures have been rederived using the most recent estimates of the peak values. Due to the premature termination of the records referenced above, some of the peak displacement values shown here are uncertain, which probably provides a partial explanation of the high degree of scatter in this parameter with respect to the best fit line. Another factor influencing the scatter is that the measured ground motion contained significant nonradial components at several of the stations. This has been interpreted by Perret (1963) to be the result of local slippage in one or more of the shear zones which were encountered during the excavation of the tunnel. Thus, what is plotted here as peak radial motion may not accurately represent the primary induced Hard Hat motion at all stations.

Figure 3-10. Surface Map of the Hard Hat Site

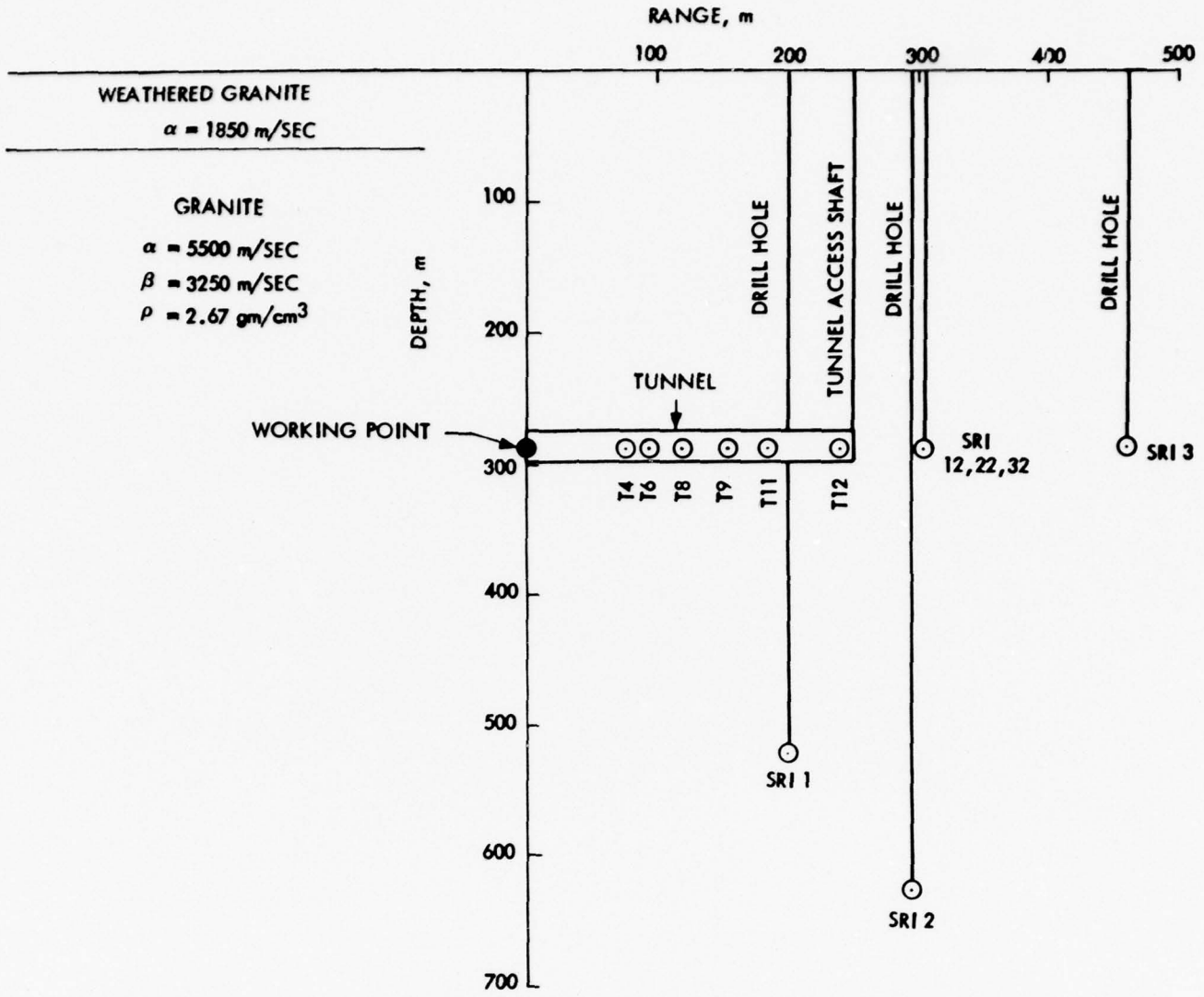

Figure 3-11. Vertical Section Through the Hard Hat Detonation Point Showing the Relationship Between the Instrument Locations and the Subsurface Geology at the Site

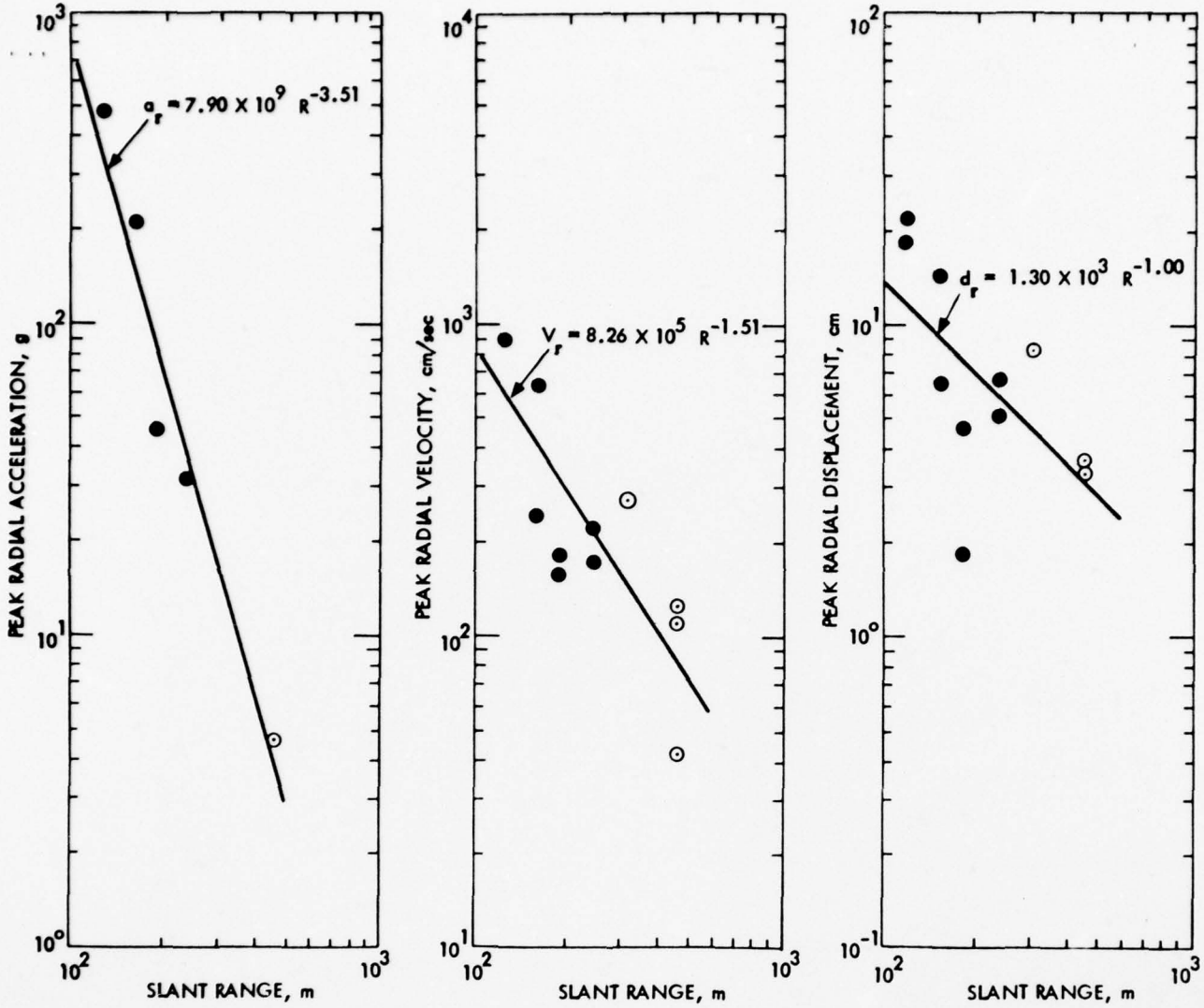

Figure 3-12. Observed Hard Hat Peak Motion Data as a Function of Range

Although at least five apparently complete radial subsurface records were obtained from this experiment (i.e., SC tunnel stations T8, T11, T12 and SRI downhole stations 2 and 3) only one RDP has been published. This is the one derived from the recording at station SRI 3 and published by Werth and Herbst (1962). However, more recently R. Bjork of Pacifica Technology has derived RDP's from the three usable SC tunnel stations and has provided copies of these data for inclusion in this report (1977). The four available RDP estimates for Hard Hat are shown together at the same scale in Figure 3-13. As with Gnome, two estimates of the potentials for Hard Hat station SRI-3 are shown in this figure corresponding to assumed compressional wave velocities of 4800 m/sec and 5863 m/sec. Werth and Herbst (1962) used the lower value of 4800 m/sec in their analysis and referenced an observed propagation velocity to this station given by Swift (1962). However, this quoted value appears to apply to the propagation velocity of the peak motion and is thus not representative of the compressional wave velocity in granite. However, as is indicated on this figure, a substitution of the higher velocity assumed by Bjork (i.e. 5863 m/sec) results in less than a 10% change in the estimated peak value of the potential at this station. In comparing the four RDP's shown in this figure it can be seen that those obtained from the three tunnel stations are all of short duration as a result of the early record termination caused by a cable break. Moreover, the peak values of the potential at these stations average about 3000 m^3 which is 50% lower than the 4500 m^3 peak value derived by Werth and Herbst (1962) at station SRI-3. There is no obvious explanation for this discrepancy, particularly in view of the fact that all four stations lie on the same azimuth. On the other hand, at the three stations at which an estimate of the static value of the potential can be made, consistent values of between 2200 and 2400 m^3 are obtained. Moreover, Werth and Herbst (1962) note that this value agrees with what would be expected on the basis of the observed final cavity radius for Hard Hat.

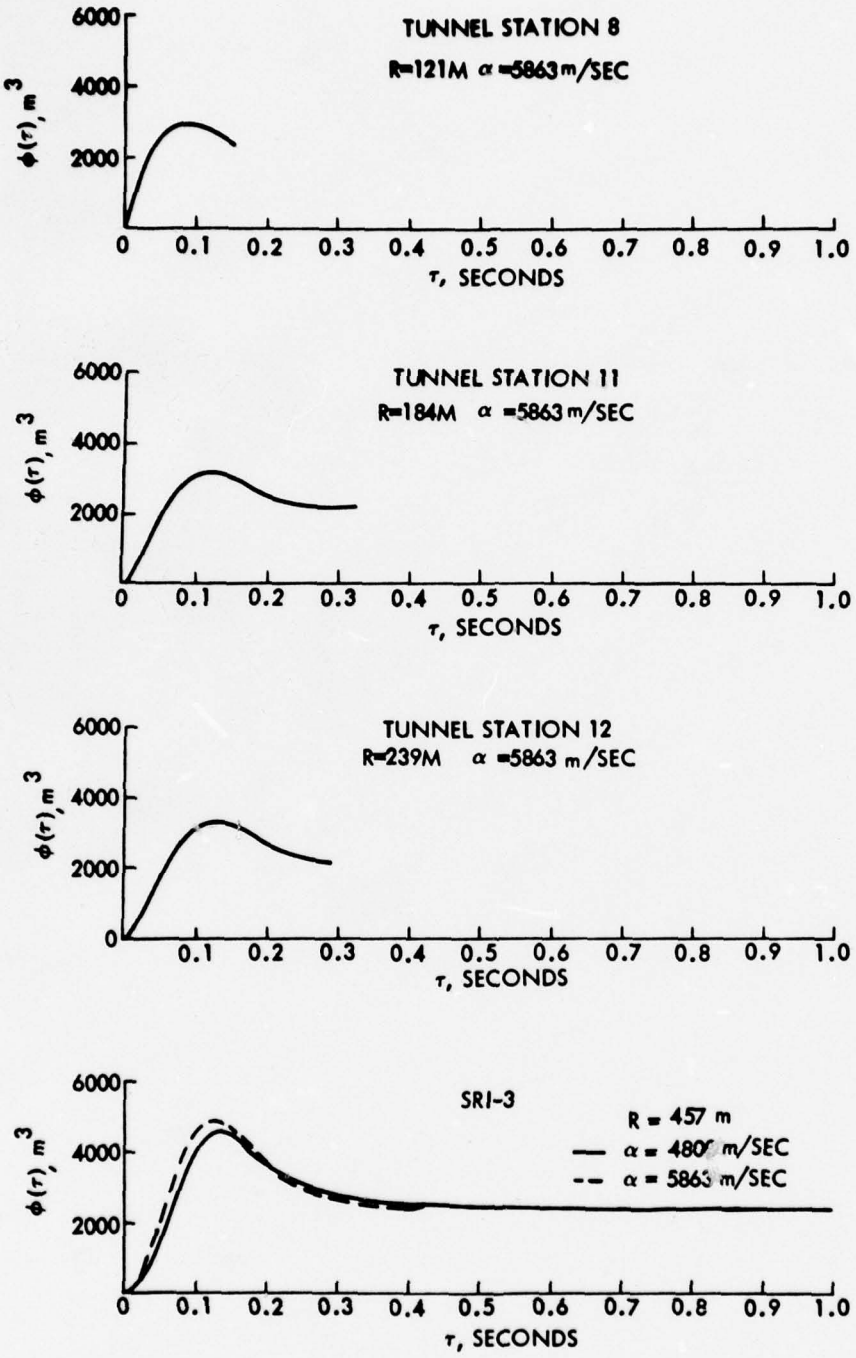

Figure 3-13. Observed Hard Hat Reduced Displacement Potentials, Stations SC-8, SC-11, SC-12 and SRI-3

3.5 SHOAL

The Shoal event was a 13 kt contained explosion which was detonated at a depth of 367 m ($h/W^{1/3}$ = 158) in the central granitic intrusive of the Sand Springs range near Fallon, Nevada on October 26, 1963. Seven shot level stations were occupied for this event; 4 in a tunnel covering the distance range from 92 to 397 m and 3 at the bottom of individual holes located at a common range of about 590 m. As in the cases of Gnome and Hard Hat, cable damage limited the duration of useful data recovered at the tunnel stations and consequently long term displacement data are available only for the three downhole stations.

Figure 3-14 is a surface map of the site (Weart, 1965) showing the locations of the tunnel shaft and three instrument holes relative to ground zero. It can be seen that the instrument holes are equally spaced azimuthally every 120^{o} around the shot point. It was originally intended that one of these stations would lie on the same azimuth as the tunnel, but this goal had to be sacrificed during the construction phase (Weart, 1965). The subsurface locations of the stations are shown projected onto a vertical plane through the shot point in Figure 3-15. As is noted on this figure, at least three fault zones of unknown vertical extent were encountered during the construction of the tunnel and while little is known about the condition of the medium along the propagation paths from the shot point to the downhole stations, it can be inferred from the tunnel experience that it is probably highly fractured. Similarly, the subsurface geologic profile indicates a massive granitic source medium extending to the surface while in fact it is known that the near surface material is highly weathered (Weart, 1965). However, the effect of this weathering on the depth dependence of the physical properties is not known at the present time.

The peak radial acceleration, velocity and displacement data observed at ranges greater than 100 m are plotted as a function of distance in Figure 3-16. As was indicated above, no peak displacement data were recovered from the tunnel stations and consequently the distance dependence of that parameter could not be determined. As with Hard Hat, there were indications of significant nonradial components of the

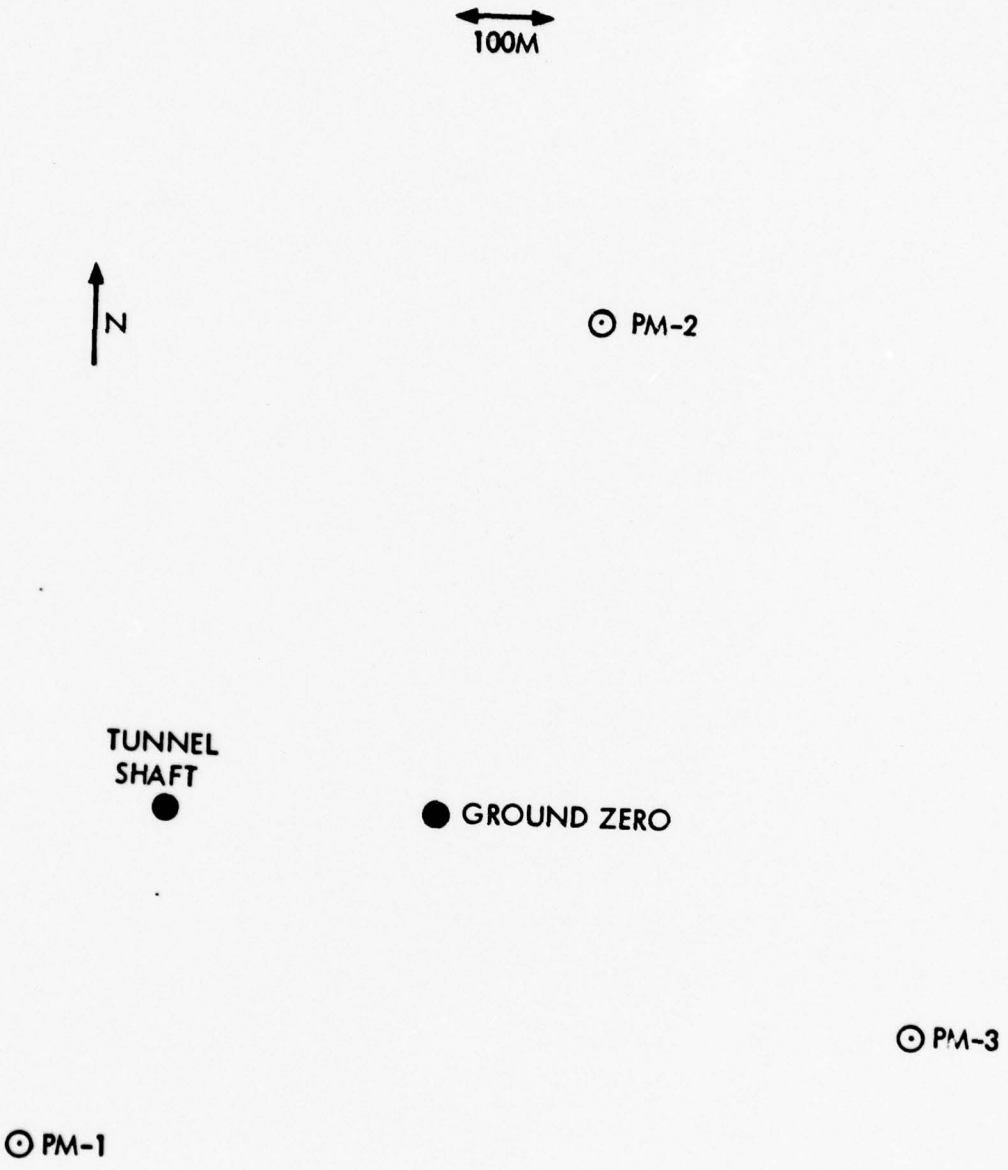

Figure 3-14. Surface Map of the Shoal Site

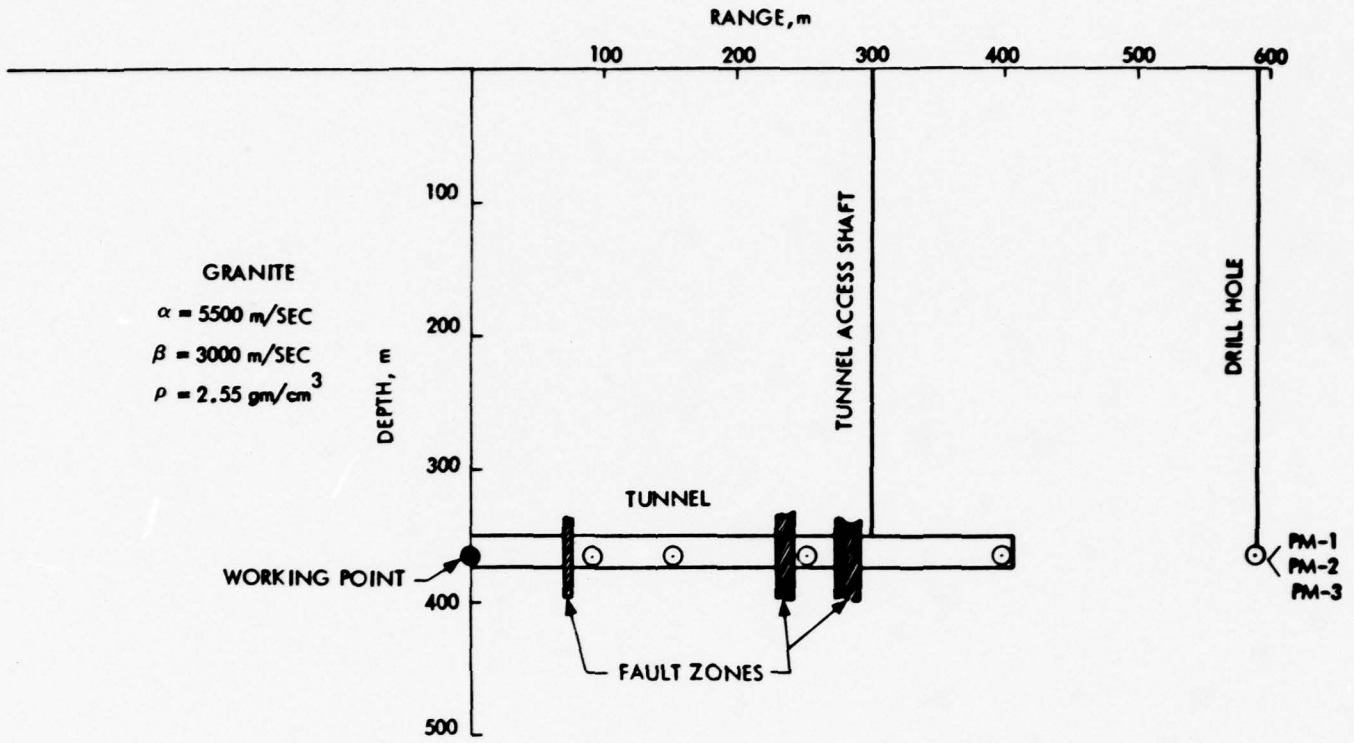

Figure 3-15. Vertical Section Through the Shoal Detonation Point Showing the Relationship Between the Instrument Locations and the Subsurface Geology at the Site

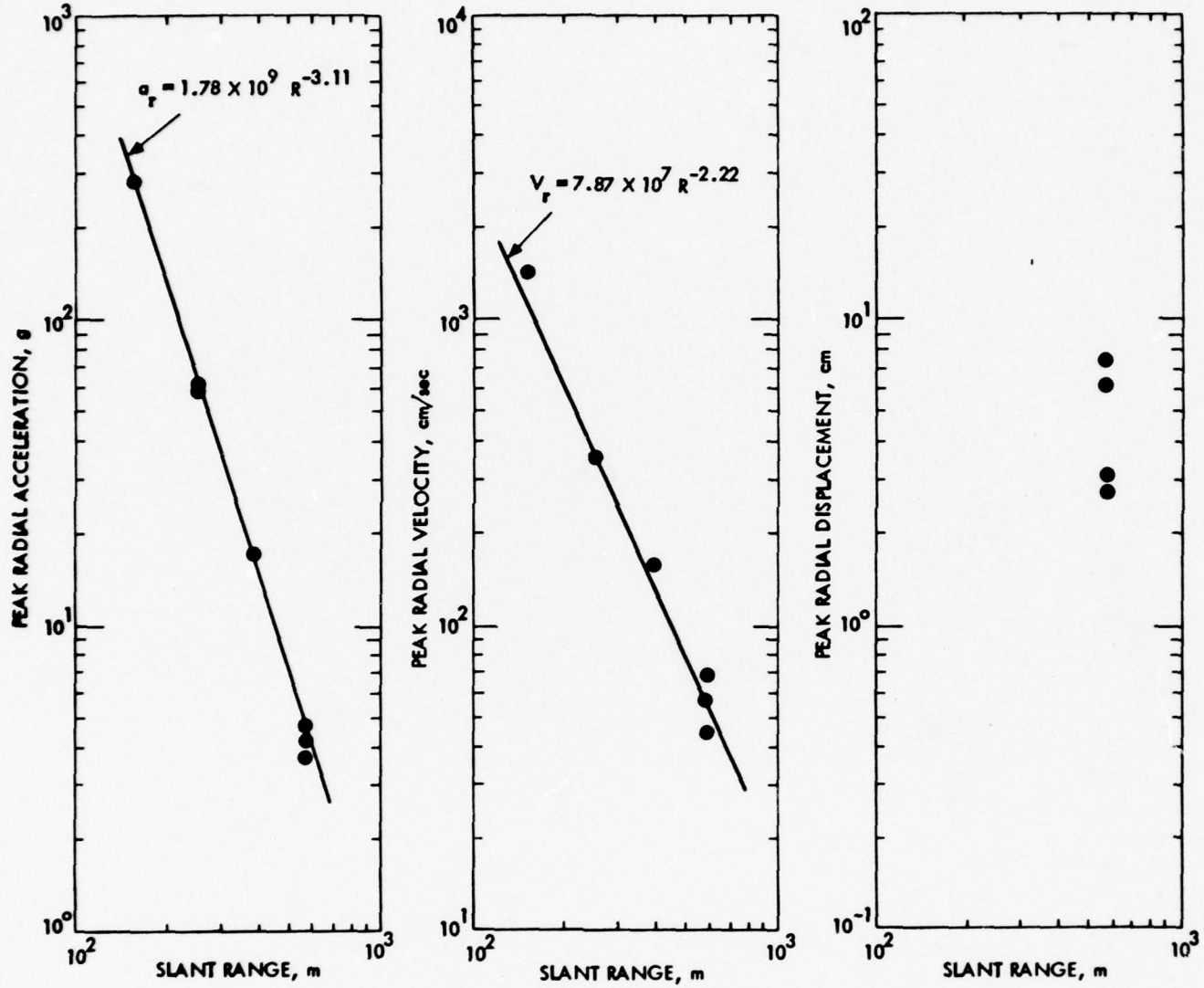

Figure 3-16. Observed Shoal Peak Motion Data as a Function of Range

motion on Shoal, even at the close-in stations. These have been interpreted by Weart (1965) to be indications of large scale block movement along zones of weakness associated with pre-existing faulting of the granitic mass. In any case, the peak motions for Shoal appear to be roughly consistent with what would be expected on the basis of Hard Hat experience.

Apparently complete radial component time histories were recovered from the three downhole stations PM-1, PM-2, and PM-3. Although the motion is clearly not purely radial at these stations, the radial component time histories have been integrated to obtain the three approximations to the Shoal RDP shown in Figure 3-17 (Weart, 1965). The observed propagation velocity to these stations of about 5,500 m/sec was apparently used in deriving these potential functions. It can be seen that these three estimates of the RDP are wildly inconsistent, with the peak value of the potential varying by more than a factor of three and the steady state value of the potentials indicating permanent radial displacements ranging from 0.3 cm inward at station PM-1 to 4.0 cm outward at station PM-3. It seems probable that this variability reflects the local block movement that was inferred above in conjunction with the peak motion data. It was noted by Weart (1965) that if the observed Hard Hat RDP published by Werth and Herbst (1962) is cube-root scaled to the Shoal yield it agrees best with the RDP from station PM-2. The observed potential peak for this station is about 7000 m^3 with an associated steady state value (at 0.9 seconds) of about 4000 m^3.

3.6 PILE DRIVER

The Pile Driver event was a 62 kt contained explosion which was detonated at a depth of 457 m ($h/W^{1/3}$ = 116) in the granite of Climax stock about 350 m east of the Hard Hat event on June 2, 1966. With regard to ground motion measurements, this was probably the most elaborately instrumented underground test at NTS with more than 100 surface and subsurface gages deployed within a 1 km radius of the detonation point. Nine of these were tunnel stations distributed over the distance range of 97 to 470 m by SC (Perret, 1968b) along a radius striking SE from the detonation

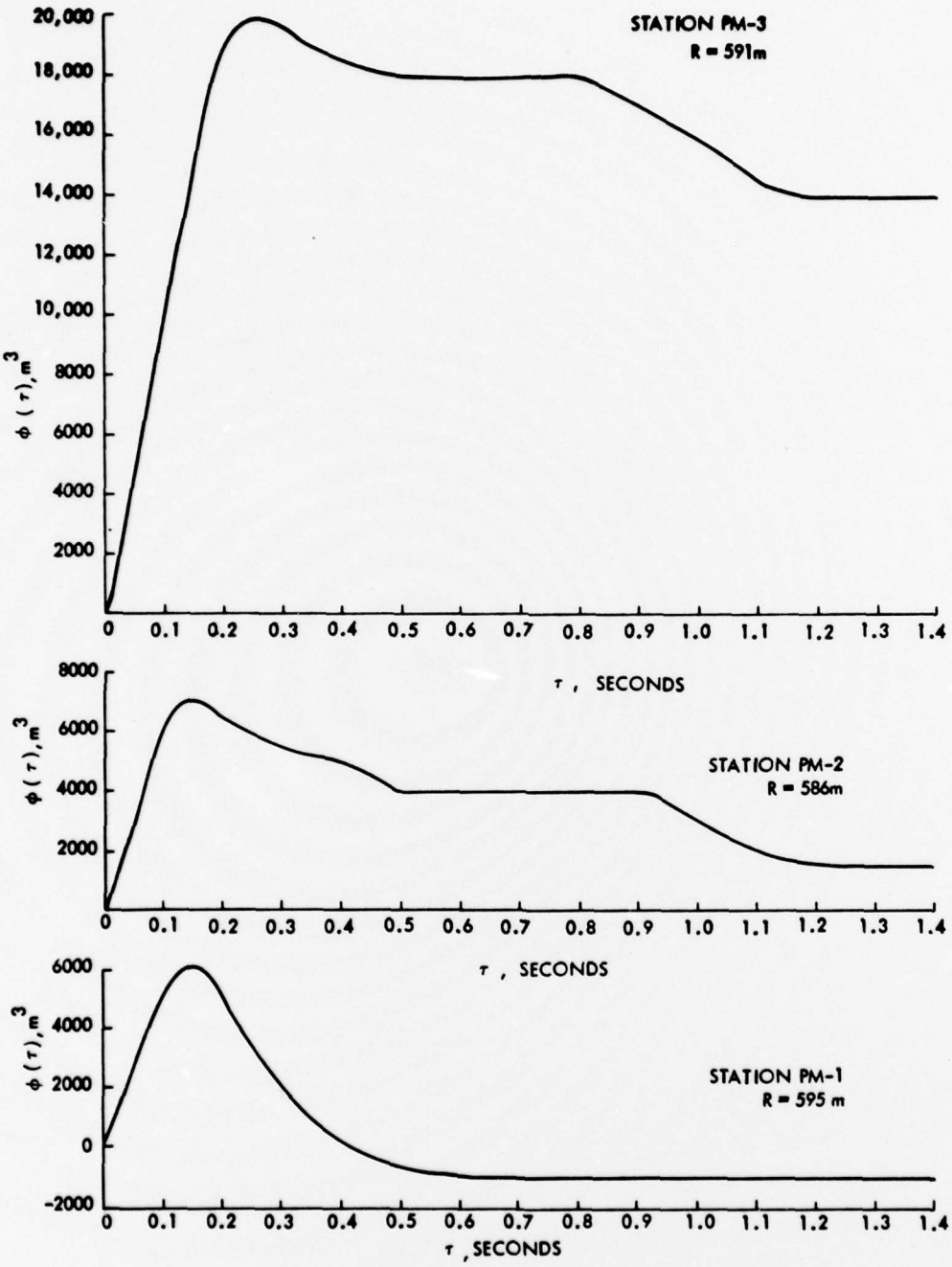

Figure 3-17. Observed Shoal Reduced Displacement Potentials, Stations PM-1, PM-2, PM-3

point. The rest of the stations were deployed on the surface and in four individual holes located at distances of about 610 and 860 m from ground zero by SRI (Hoffman and Sauer, 1969). The objectives of the ground motion monitoring were ambitious and included efforts designed to (1) study surface spalling and its contribution to downward-travelling energy, (2) determine the source function for teleseismic signals along a line bearing N58^{o}E from the shot and (3) investigate the subsurface ground motion transition across the Boundary Fault between the Climax stock and Yucca Valley. Unfortunately, almost all the expected data were lost as a result of cable breaks and instrument malfunctions and, as a result, the objectives of the experiment were only partially satisfied.

Figure 3-18 is a surface map of the site (Hoffman and Sauer, 1969) showing the locations of the tunnel shaft, the four instrument holes and the surface trace of the Boundary Fault relative to ground zero. It can be seen from this figure that the tunnel is located on a radius striking about S40^{o}W from ground zero while the instrument holes are distributed along two lines; one striking about N60^{o}E, the other S60^{o}E. It appears from this map that both stations SRI-24 and SRI-25 lie east of the Boundary Fault in Yucca Valley. In fact, due to the local dip of the fault, the shot depth station SRI-24-3 is in granite while shot depth station SRI-25-3 is in tuff. More details concerning the geometry of this environment will be shown in a subsequent figure.

The subsurface locations of those stations which recorded usable data are shown projected onto a vertical plane through the shot point in Figure 3-19. As is noted on the figure, a fault zone was encountered during the construction of the tunnel and additional instruments were installed on either side of this one in order to assess its effect on the outgoing signal (Perret, 1968b). The subsurface geologic profile shown on the left of this figure appears to be a reasonable approximation for all the stations except SRI-24-3 and SRI-25-3. As with Hard Hat, a thin low velocity surface layer has been added to account for the observed decrease in propagation velocity to the shallower stations. The best estimate of the subsurface geology along a vertical section through stations SRI-24-3 and SRI-25-3 is shown in Figure 3-20.

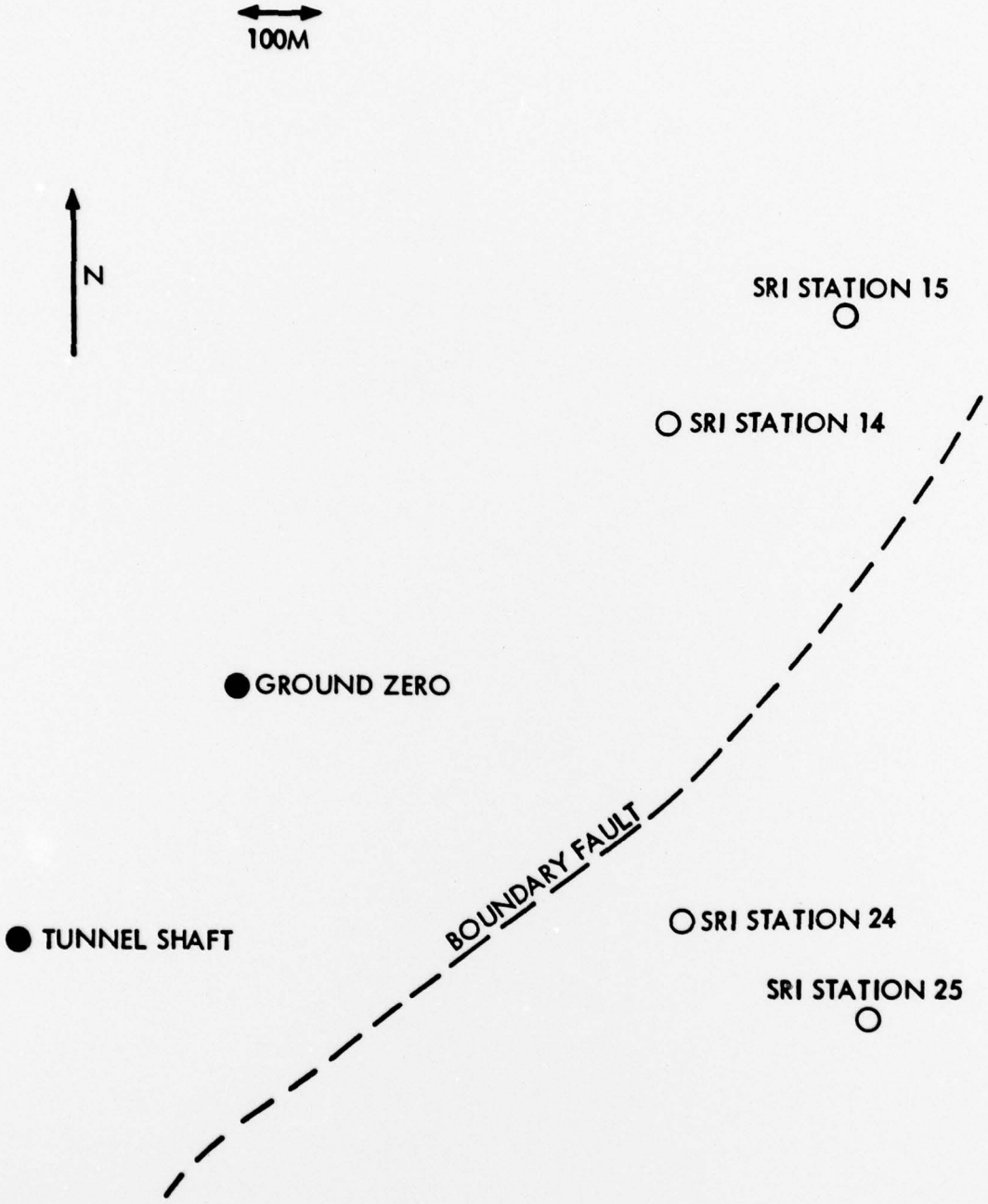

Figure 3-18. Surface Map of the Pile Driver Site

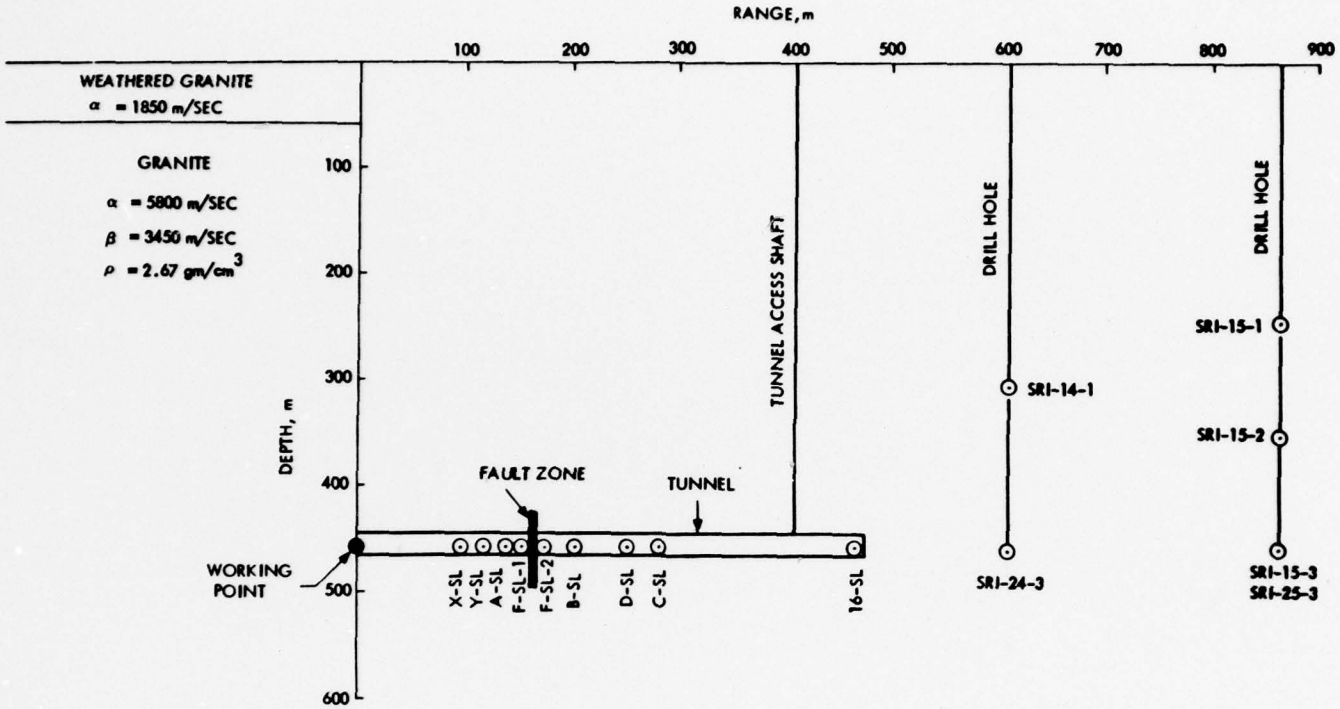

Figure 3-19. Vertical Section Through the Pile Driver Detonation Point Showing the Relationship Between the Instrument Locations and the Subsurface Geology at the Site

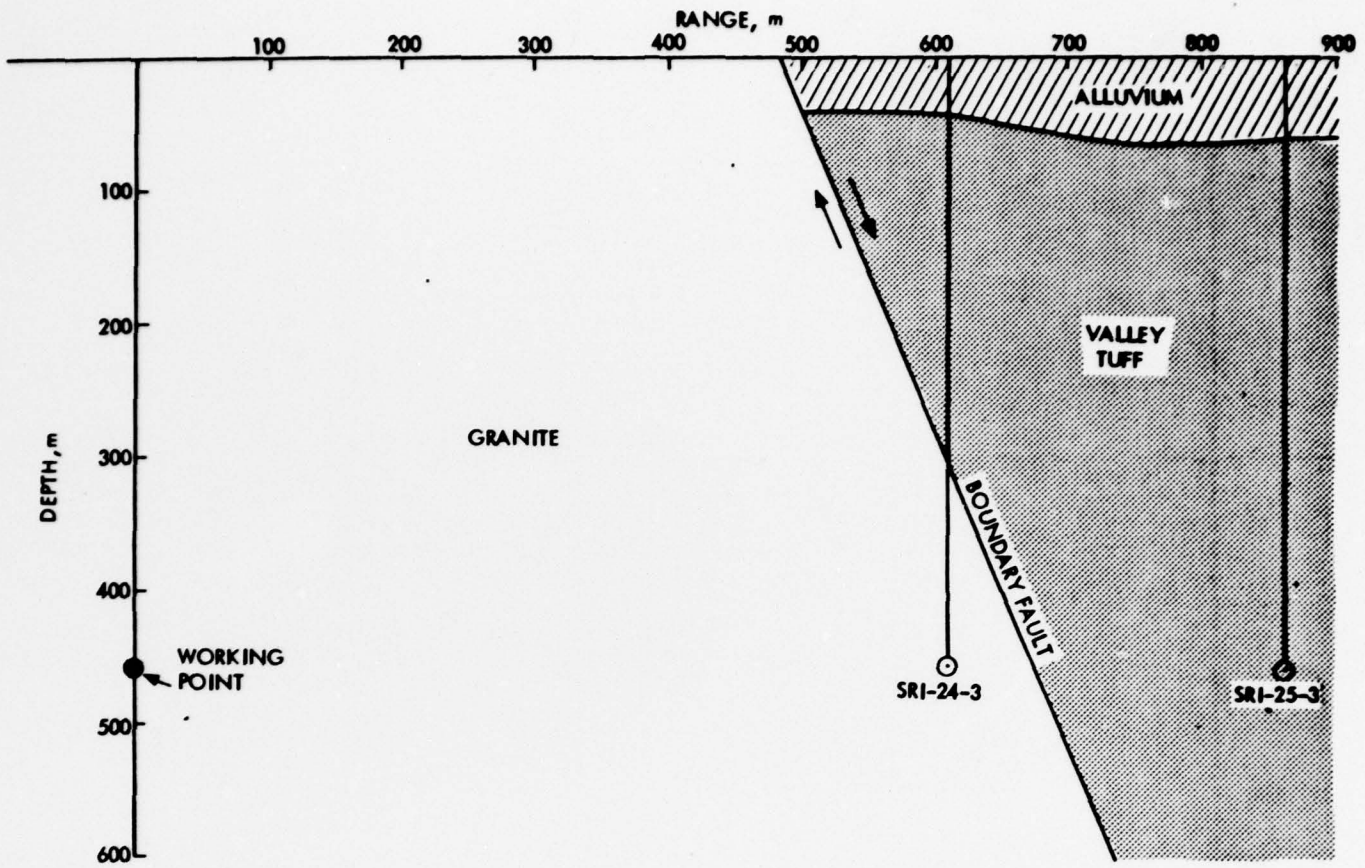

Figure 3-20. Vertical Section Through the Pile Driver Detonation Point Showing the Locations of Stations SRI-24-3 and SRI-25-3 with Respect to the Boundary Fault

Due to the instrumentation problems referenced above, complete records were recovered only from two of the tunnel stations (B-SL and 16-SL) and none of the SRI stations below shot level recorded usable data. The few peak radial acceleration, velocity and displacement data which were recovered are plotted as a function of distance in Figure 3-21. Again, the SC data (Perret, 1968b) are shown as solid circles and the SRI data (Hoffman and Sauer, 1969) as open circles. The solid lines are Perret's (1968b) least-squares fits to his tunnel data. No fit to the peak displacement values was given since data were recovered at only two tunnel stations. The SRI peak acceleration data are clearly not consistent with a projection of Perret's fit to greater distances, but it is difficult to attach much significance to this fact given the poor quality of the available records. Perret (1968b) concluded that the Pile Driver peak accelerations and velocities recorded in the tunnel are consistent with the corresponding scaled Hard Hat data but that the close-in Pile Driver peak displacements are more than a factor of two larger than what would be expected on the basis of Hard Hat experience. Clearly, such conclusions have to be regarded as tentative given the small sample of data which is available for analysis.

Apparently complete radial component time histories were recorded at five stations: tunnel stations B-SL (200 m) and 16-SL (470 m) and shot level SRI stations SRI-24-3 (610 m), SRI-25-3 (863 m) and SRI-15-3 (863 m). Neither Perret (1968b) nor Hoffman and Sauer (1969) published RDP's derived from these data, but subsequent analyses have been performed by other investigators. Bjork (1977) has provided his estimates of the RDP's from tunnel stations B-SL and 16-SL and Cherry et al (1973) have published estimates of the RDP's for the three SRI stations. These are shown on a common scale in Figures 3-22 and 3-23. It appears that they were all computed assuming the observed Pile Driver compressional wave velocity of about 5800 m/sec. The two potentials provided by Bjork (1977) were terminated at 0.7 seconds and the dashed lines on these two figures correspond to the steady state value of the potential which would be expected on the basis of the observed permanent displacements at these stations (Perret, 1968b). It should also be noted that most estimates of the elastic radius for this event would suggest that both of these stations are located within

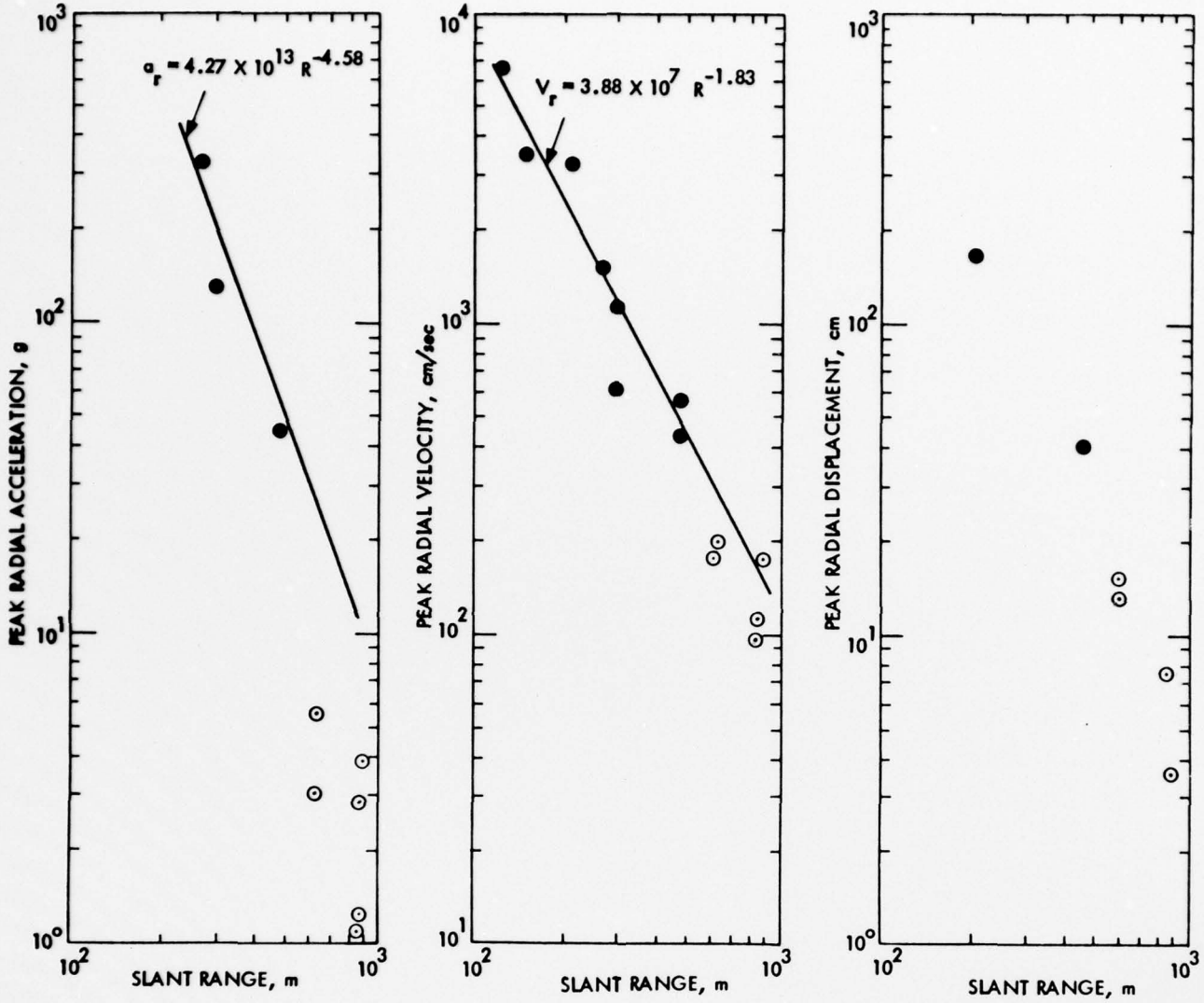

Figure 3-21. Observed Pile Driver Peak Motion Data as a Function of Range

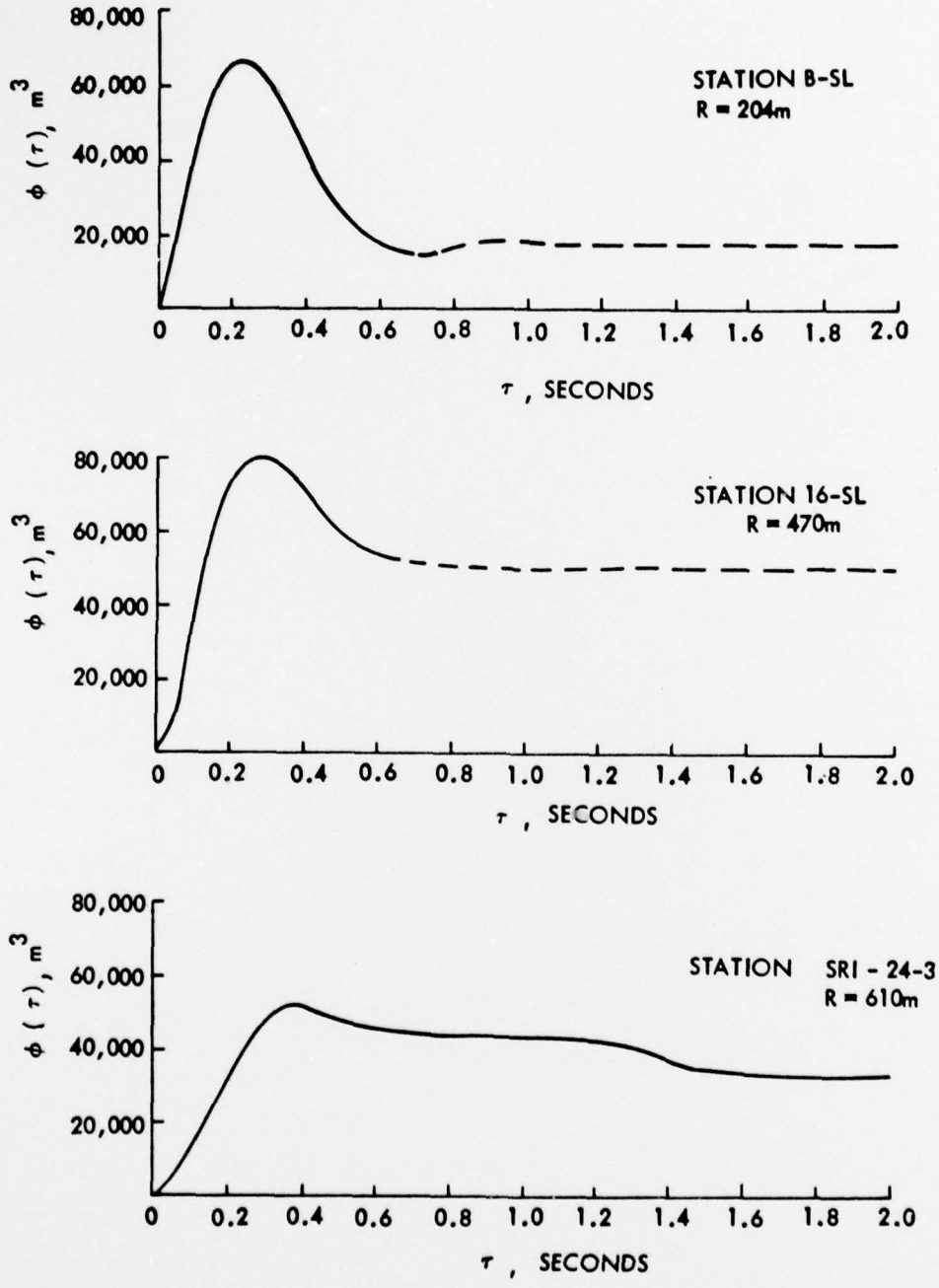

Figure 3-22. Observed Pile Driver Reduced Displacement Potentials, Stations B-SL, 16-SL and SRI-24-3

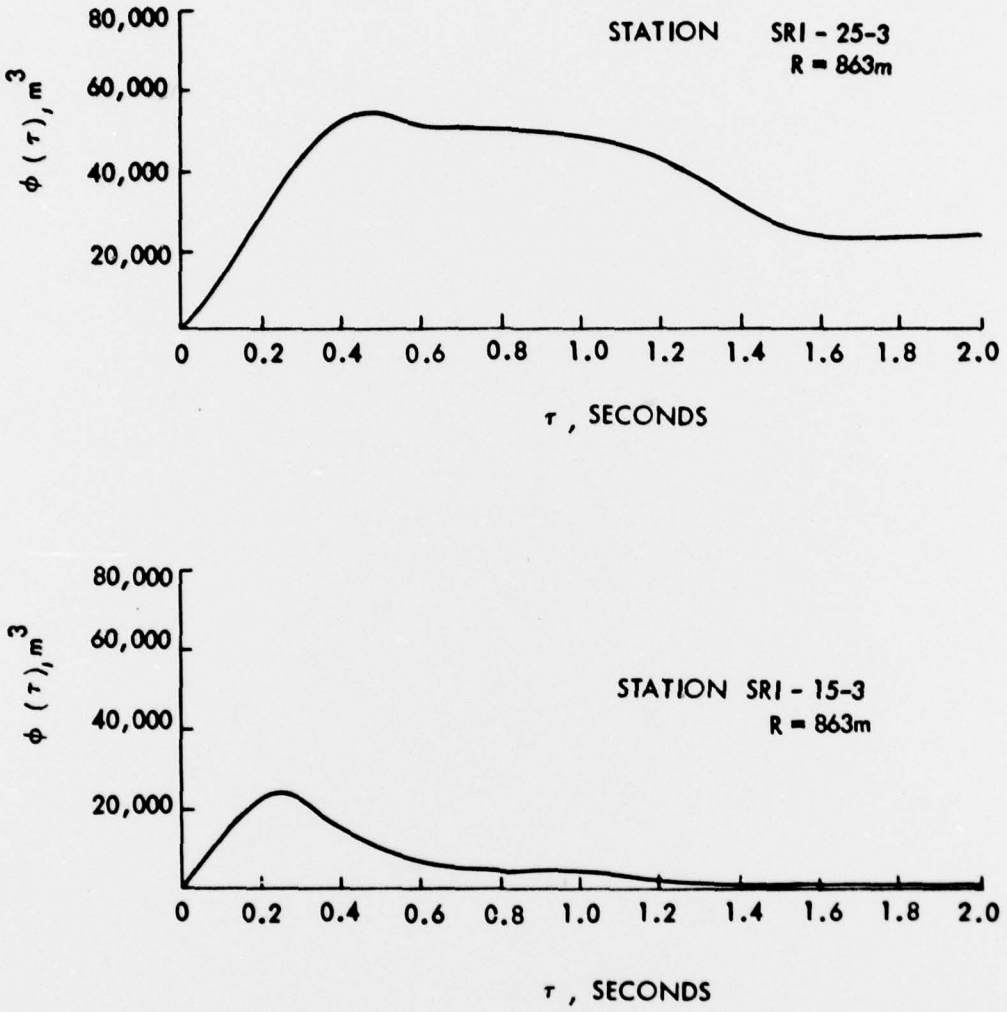

Figure 3-23. Observed Pile Driver Reduced Displacement Potentials, Stations SRI-25-3 and SRI-15-3

the nonlinear regime. As with the other granite data, there is a great deal of scatter in these RDP's with the peak value ranging from about 20,000 to nearly 80,000 m^3 and the residual value ranging from essentially zero to as much as 50,000 m^3. By way of comparison, cube-root scaling of the Hard Hat RDP's to the Pile Driver yield suggests a peak value in the 30,000 to 50,000 m^3 range and a residual value of about 20,000 m^3. It is interesting to note in comparing the individual RDP's on Figures 3-22 and 3-23 that the most consistent pair are those derived from data recorded at stations SRI-24-3 and SRI-25-3 which are located in completely different media on opposite sides of the Boundary Fault.

CHAPTER 4 - SUMMARY AND RECOMMENDATIONS FOR FURTHER STUDY

The investigation summarized in this report has centered on an attempt to collect and organize the available free-field ground motion data from U. S. tests in salt and granite. The primary objective of the study has been to reformat the published data into a homogeneous form which will serve as a useful reference for researchers who are attempting to define theoretical seismic source functions for contained explosions in these two media.

In Chapter 2 the general characteristics of subsurface ground motion data were discussed and effects due to the presence of the free surface and departures from homogeneity were analyzed in a preliminary fashion. In particular, it was demonstrated that the interpretation of measurements taken above shot depth is complicated by the presence of the free surface and that this effect can lead to significant overestimates of the steady state value of the RDP. Perturbations due to departures from homogeneity were found to increase with increasing distance from the source, in agreement with what would be expected when the distance dependence of the travel paths of the direct and reflected arrivals is considered.

The available free-field data measured from the Gnome and Salmon events in salt and the Hard Hat, Shoal and Pile Driver events in granite were summarized in Chapter 3. Subsurface geologic profiles were presented for each event to illustrate the environment in which the measurements were made. A total of 20 RDP's have been reproduced: 7 from Salmon, 1 from Gnome, 4 from Hard Hat, 3 from Shoal and 5 from Pile Driver. In general, the salt data appear to be quite consistent while the granite data show large inconsistencies both between events and for different stations monitoring the same events. Various previous investigators have attributed this variability to large scale block movement in the highly fractured granites, and no better explanation seems to be available at the present time.

In summary, the objectives of this investigation have been at least partly met in that a variety of published and previously unpublished free-field data measured from explosions in salt and granite have been integrated into a homogeneous data base. It is therefore recommended that this effort be continued and expanded to cover the compilation of free-field data measured from explosions in other media of interest. Such data are likely to play an important role in the evaluation of any data exchange packages which may be associated with future test ban treaties.

REFERENCES

Bjork, R. L., 1977, Personal Communication.

Cherry, J. T., C. B. Archambeau, T. C. Bache, and D. G. Harkrider, 1973, "The Teleseismic Radiation Field From Explosions: The Dependence of M_s and m_b on Earth Structure and Near Source Environment," SSS-R-73-1834.

Haskell, N. A., 1967, "Analytic Approximation for the Elastic Radiation from a Contained Underground Explosion," J. Geophys. Res. 72, 2583.

Hoffman, H. V. and F. M. Sauer, 1969, "Shot Pile Driver: Free-Field and Surface Motions" PϕR-4000.

Murphy, J. R., 1972, "Calculated Compressional Wave Arrivals From Underground Nuclear Detonations," BSSA, 62, 991.

Patterson, D. W., 1966, "Nuclear Decoupling Full and Partial" J. Geophys. Res. 71, 3427.

Perret, W. R. 1963, "Shot Hard Hat: Free-Field Ground Motion Studies in Granite," POR-1803.

Perret, W. R., 1968a, "Free-Field Particle Motion From a Nuclear Explosion in Salt, Part I, Project Dribble, Salmon Event" VUF-3012.

Perret, W. R., 1968b, "Shot Pile Driver: Free-Field Ground Motion in Granite" POR-4001.

Rogers, L. A., 1966, "Free-Field Motion Near a Nuclear Explosion in Salt: Project Salmon" UCRL - 14463.

Springer, D. L. 1966, "Calculation of First-Zone P Wave Amplitudes For the Salmon Event and for Decoupled Sources," J. Geophys. Res., 71, 3459.

Swift, L. M , 1962, "Hard Hat Event: Measurement of Close-In Earth Motion," VUP - 2101.

Swift, L. M., 1963, "Project Gnome: Intermediate Range Earth Motion Measurements," PNE - 111F.

Swift, L. M. and J. D. Eisler, 1965, "Antler and Hard Hat Events: Measurement of Close-In Earth Motion," VUF - 2100.

REFERENCES (Cont'd)

Tien, J. H., and F. A. Hadsell, 1970, "Remnant Radial Strain in a Half-Space From an Isotropic Source," BSSA, 60, 1017.

Weart, W. D., 1963, "Project Gnome: Particle Motion Near a Nuclear Detonation in Halite," PNE - 108F.

Weart, W. D. 1965, "Project Shoal: Free-Field Earth Motion and Spalling Measurements in Granite," VUF - 2001.

Werth, G. C. and Roland F. Herbst, 1962, "Comparison of Amplitudes of Seismic Waves From Nuclear Explosions in Four Media," UCRL - 6962.